5-2012

An Investigation of the use of Ceramic Microencapsulated Fuel for Transuranic Waste Recycling in Pressurized Water Reactors

Cole Andrew Gentry
Cole-Gentry@utc.edu

To the Graduate Council:

I am submitting herewith a thesis written by Cole Andrew Gentry entitled "An Investigation of the use of Ceramic Microencapsulated Fuel for Transuranic Waste Recycling in Pressurized Water Reactors." I have examined the final electronic copy of this thesis for form and content and recommend that it be accepted in partial fulfillment of the requirements for the degree of Master of Science, with a major in Nuclear Engineering.

Guillermo I. Maldonado, Major Professor

We have read this thesis and recommend its acceptance:

Laurence F. Miller, Jess C. Gehin

Accepted for the Council:
Dixie L. Thompson

Vice Provost and Dean of the Graduate School

(Original signatures are on file with official student records.)

An Investigation of the use of Ceramic Microencapsulated Fuel for Transuranic Waste Recycling in Pressurized Water Reactors

A Thesis Presented for the
Master of Science
Degree
The University of Tennessee, Knoxville

Cole Andrew Gentry
May 2012

Dedication

I wish to dedicate this thesis to my friends and family, especially

My mom and stepdad, Connie and Harry Uffalussy, for their loving guidance, and keeping me straight

My dad, Steve Gentry, for always listening when I needed someone to talk to

My girlfriend, Ashley Swiderski, for the love, patience, and home cooked meals

My friends Andrew, John, and Richie, for their honest opinions and the laughs

Acknowledgements

I wish to show my appreciation to Dr. Ivan Maldonado, for the opportunities and the mentorship he has provided me through my graduate school career thus far.
Also, I would like to thank Dr. Jess Gehin, Dr. Kurt Terrani, and Andrew Godfrey, for their mentorship and guidance throughout this entire project, without whose help this would not be possible.

I would like to express my gratitude towards Brian Ade, Matt Jessee, and others of the ScaleHelp team for the time taken to assist us in using SCALE for this study, as well as Hermilo Hernandez-Noyola for his guidance with NESTLE. They all took time outside of their normal working schedules to help with any questions or issues encountered, and their input and assistance has been invaluable.

I thank my dissertation committee Dr. Ivan Maldonado, Dr. Jess Gehin, and Dr. Laurence Miller, for their help with the completion of this thesis.

I would finally like to thank my friends and family for their loving support and for always being there when I needed them.

Abstract

Presented is an investigation of the utilization of Tristructural-Isotropic (TRISO) particle-based fuel designs for the recycling of Plutonium/Neptunium (Pu/Np) Transuranic (TRU) isotopes in typical Westinghouse four-loop pressurized water reactors. Though numerous studies have evaluated the recycling of TRU isotopes in light water reactors (LWRs), this work differentiates itself by employing Pu/Np loaded TRISO particles embedded within a SiC matrix and formed into pellets that can be loaded into standard 17x17 fuel element cladding. This approach provides the capability of Pu/Np recycling, and by virtue of the TRISO particle design, will allow for greater burnup of Pu/Np material and improved fuel reliability. In this study, a variety of assembly layouts and core loading patterns were analyzed to demonstrate the feasibility of Pu/Np loaded TRISO fuel. The assembly and core designs herein reported are not fully optimized, and require fine-tuning to flatten power peaks, however, the progress achieved thus far strongly supports the conclusion that with further rod/assembly/core loading and placement optimization, Pu/Np loaded TRISO fuel and core designs that are capable of balancing Pu/Np production/destruction can be designed within the standard constraints for thermal and reactivity performance in PWRs.

Table of Contents

List of Tables

List of Figures

1. Introduction and General Information

1.1. Nuclear Waste Generation

One of the primary issues currently facing the nuclear industry is the management of waste material generated by the burning of nuclear fuels. In typical Light Water Reactors (LWRs), which are the primary operating commercial designs used in the United States, uranium oxide (UO_2) fuel pellets are fabricated into fuel assembly lattices or bundles, and then burned in a reactor for a time frame of approximately 4.3 years (i.e. three full length operating cycles). The UO_2 pellets are enriched such that 3.0 - 5.0 wt% of the uranium is U-235, with the remaining uranium mostly being U-238 (some trace amounts of other uranium isotopes are present as well). As the fuel is exposed to the high neutron flux of the reactor, some of the fuel fissions to generate the primary source of thermal energy used in the electrical power generation, whereas the remainder is either unaffected by the neutrons, or is transmuted into other isotopes or elements. Of the transmuted isotopes, those of most significance to the nuclear waste dilemma are the Transuranics (TRU) which can be long lived and generate substantial heat from their radioactive decay. However, some TRU waste consists of fissile isotopes (isotopes that readily fission when interacting with thermal spectrum neutrons) which can be recycled and reused as a potential alternative source of fuel material. Of the TRU isotopes, Pu-239 and Pu-241 are two of the more notable fissile isotopes for use as fuel. These two fissile isotopes make up a fairly significant quantity of the plutonium present in spent fuel, and only requires chemical separation from other waste material for it to be useable as a fuel source (i.e. no isotopic enrichment is required)

1.2. Transuranic Material Recycling

The concept of recycling Transuranic (TRU) material as a means of reducing waste or nuclear weapons Plutonium inventory and providing an additional source of fuel material for Light Water Reactors (LWRs) has been a well studied topic and is a current practice in several countries. Several countries have used MOX based fuels, or fuel designs that use a mix of PuO_2 and UO_2, for several years and have optimized their designs such that their overall performance is similar to that of UO_2 fuel. The experience with MOX in PWRs has been positive with no outstanding or unresolved operational safety issues [3]. The United States does not currently practice spent fuel reprocessing on a large commercial scale primarily due to its lack of economic competitiveness [4], but with ever increasing uranium and storage costs, the desire to dispose of plutonium weapons stockpiles, along with technological advancements in the reprocessing method, it is expected that the United States will eventually adopt fuel reprocessing as a common practice. For countries that do practice spent fuel or weapons reprocessing, plutonium is primarily separated from spent fuel via the PUREX process and can then be loaded into fuel in any desired fabrication method, though the only method currently employed is the MOX approach [5].

Some of the more recent studies of advanced Light Water Reactor (LWR) fuel designs include the Combined Non-Fertile and UO_2 (CONFU) inert matrix based fuel concept and the COmbustible Recyclable A ILot (CORAIL) Mixed Oxide (MOX) based fuel concept [1,2]. Research is also being conducted on the use of alternative reactor designs such as the Modular Helium Reactor and Sodium-cooled Fast Reactor as

alternative means of waste recycling (NOTE: this manuscript focuses on the analysis of LWR fuel concepts) [27,29].

1.3. Deep Burn Concept

One significant disadvantage of current MOX designs is that MOX fuel elements require multiple recycling to achieve substantial burn-up of the plutonium material, and this multiple recycling process becomes more expensive with each recycling pass [6]. The Deep Burn concept, or the concept of developing plutonium-based fuels capable of sustaining high levels of burn-up of the plutonium, was proposed as a solution to this problem [7]. Basic Deep Burn fuel designs center around using TRistructural ISOtropic (TRISO) particles, which are small multilayered particles used to contain fuel and fission products. An Illustration of this along with brief descriptions of the purposes for each layer is provided in Figure 1.

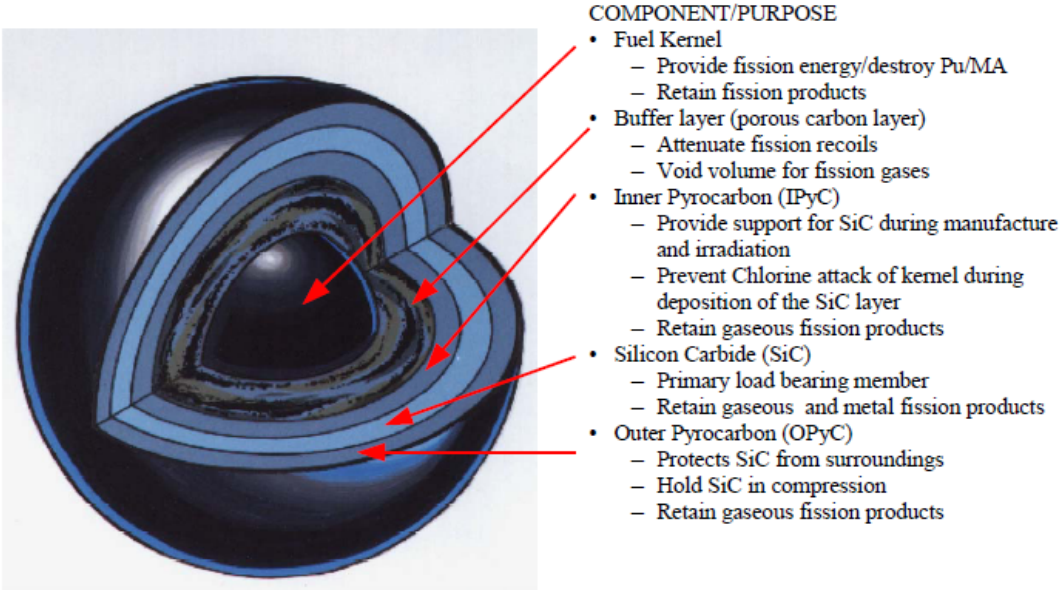

Figure 1 Functional Schematic of TRISO-coated Particle [7]

TRISO particles kernels are fabricated using a gel formation process where spherical kernels are formed from aqueous metal solutions. The process consists of passing a solution containing heavy metal nitrates through vibrating needles creating a small droplet that is then gelled through various chemical reactions and are then washed, dried, and sintered to form the dense ceramic kernels [8]. Coatings are then applied using chemical vapor deposition in a high-temperature fluidized bed [9]. After forming the TRISO particles, they can be mixed into various material structures (i.e. matrix materials) depending upon the desired application. Presently, TRISO particles have been fabricated and irradiated with uranium, thorium, and plutonium based fuel kernels [7]. Though fabrication and irradiation has yet to be demonstrated with Pu/Np or TRU based kernels, it is expected that this should be possible and with comparable results.

This concept was originally developed for use in high temperature gas-cooled reactors in which the TRISO particles would be dispersed within a graphite matrix but has since been adapted for use in Light Water Reactor fuel elements using a silicon carbide matrix. The SiC matrix improves irradiation stability, provides another effective barrier to fission product release, performs with greater reliability under the anticipated operating and long-term storage conditions, and provides greater resistance towards proliferation. This fuel design of TRISO particles mixed within a SiC matrix is known as a Fully Ceramic Microencapsulated (FCM) fuel design. The SiC matrix material, fabricated using the Nano-Infiltration and Transient Eutectic-phase (NITE) process, is mixed with TRISO particles in a graphite die, and is then hot pressed to form a fuel pellet

[10]. These pellets may then be loaded into a fuel assembly in the same manner as typical UO_2 fuel as illustrated in Figure 2

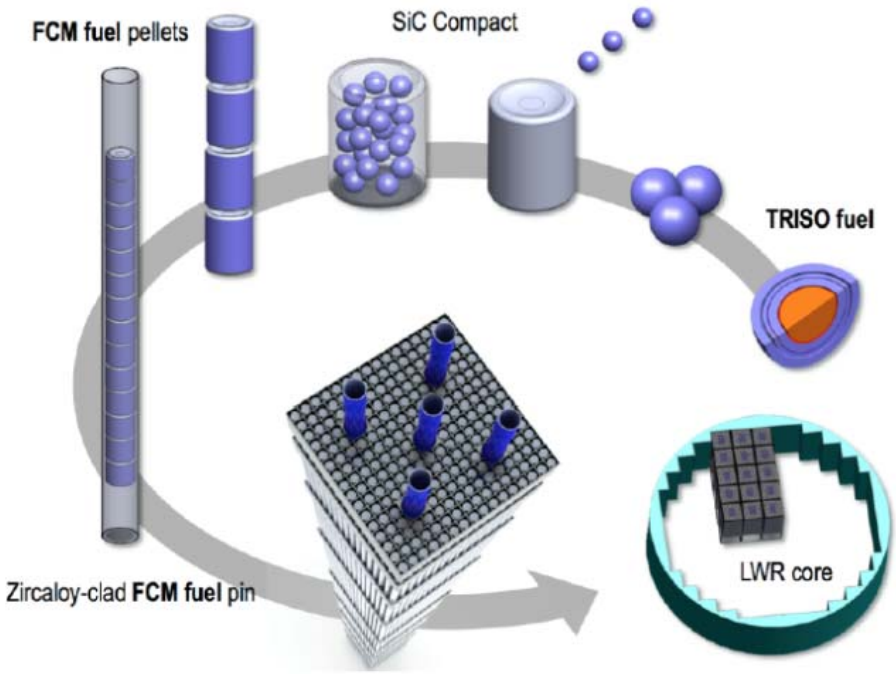

Figure 2 FCM fuel manufacturing process for LWRs [11]

Manufacturing fuel in this manner, as opposed to the typical MOX process, provides a number of advantages. Firstly, FCM fuel is capable of achieving a higher burnup of the plutonium and other fissile material in a single pass which reduces, if not eliminates, the requirements for multiple separations and re-fabrications of the fuel after the initial recycling and reduces the inventory of TRU material in the fuel cycle. Secondly, the coating of the fuel particles should provide additional confinement of the residual TRU material and fission products such that the FCM rods will be safer than typical MOX rods in both operation and long-term storage [7].

1.4. Research Goals

Currently, research is already underway with other groups for designing LWR fuels that can utilize the TRISO technology for TRU recycling [11,12]. However, this work is still in progress, and so it is believed that contributions can still be made towards the progression of this research via computer model simulations. Therefore, the ultimate goal of this herein presented research is to devise and demonstrate (via simulation) a fuel assembly and full core design that reasonably mimics the same behaviors of a typical LWR fuel and core design, while utilizing FCM fuel to recycle isotopes of Np-237, Pu-238, Pu-239, Pu-240, Pu-241, and Pu-242 such that the amount of production and destruction of the sum of these isotope masses is balanced at the end of each operating cycle on both the assembly and core level. Balancing the sum of the selected Pu/Np isotopes in this manner ensures that on the assembly and core level, no additional waste of these isotopes is generated at the end of each cycle and assembly discharge.

This research focuses on the neutronic design of the fuel and core based the most important parameters; namely, reactivity behavior, relative power peaking, fuel burnup, and isotopic concentrations. Additional future work requires the analysis of thermal stresses and loads, adverse condition tolerance, chemical behaviors, and a number of other factors. Also, based on the existing research found already, it is believed that a Pressurized Water Reactor (PWR) core and fuel design would provide the most contribution to field of LWR FCM fuels as it stands presently.

1.5. Description of Basis Assembly and Core Designs

There are a number of different PWR reactor and fuel assembly designs to use as a basis design from which to start with, but one of the more typical of these designs in the United States is the 4-Loop Westinghouse 193 assembly PWR core that uses a 17 x 17 assembly design Illustrated in Figure 3 and Figure 4.

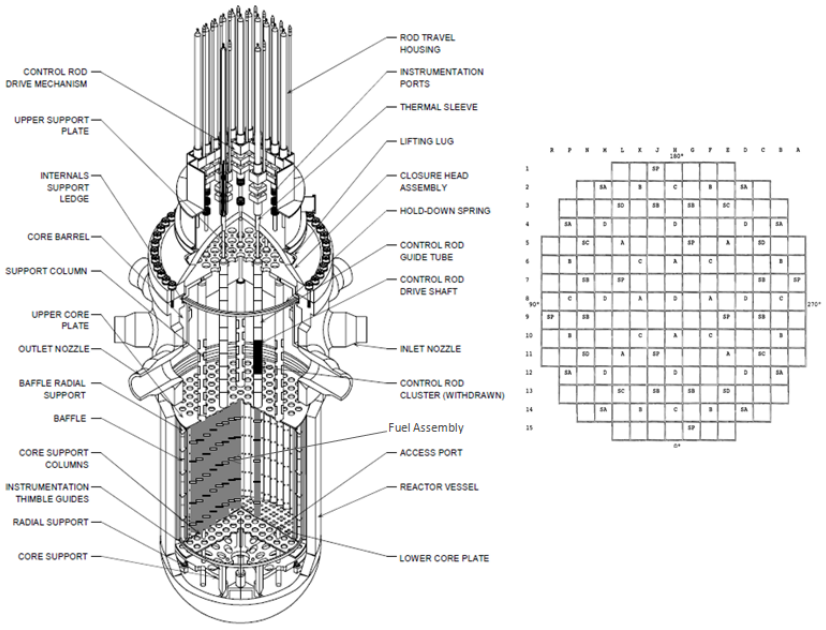

Figure 3 Westinghouse 4-Loop 193 Assembly Core [13,14]

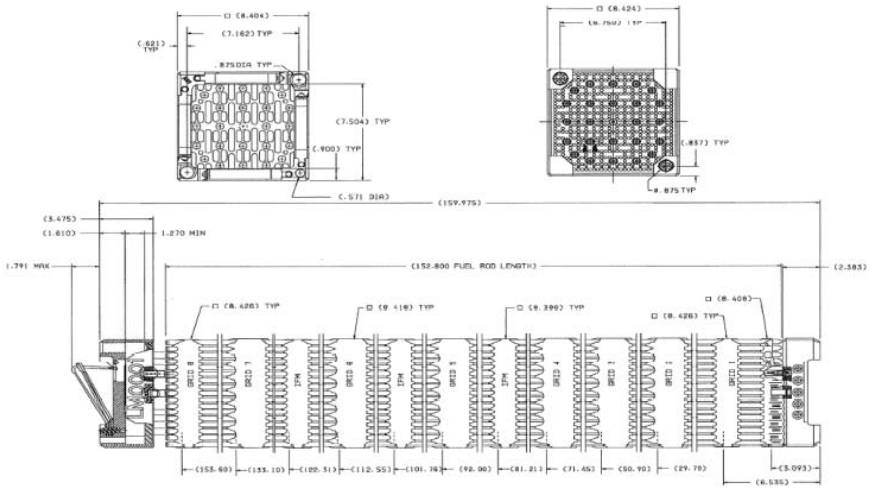

Figure 4 Westinghouse 17x17 Fuel Assembly [14]

Because they are fairly typical and representative of modern PWRs, this core and assembly design combination was chosen as the basis for the design goals of this research. The core consists of 193 fuel assemblies placed side by side to form a nearly cylindrical configuration (see Figure 3 top down assembly arrangement of illustration). Each assembly consists of 264 fuel rods arranged in a 17x17 array with 24 locations being designated as control rod guide tubes locations for control rods or fuel inserts to slide into and 1 center instrument tube location intended for in-core detector instruments. Fuel assemblies may or may not use Burnable Poisons (BP), which are materials that readily absorb neutrons and prevent them from interacting with fuel to produce fission. Burnable poisons of some sort are typically required in fresh fuel assemblies to control assembly power peaking and are usually loaded with different concentrations and or number of poisoned elements depending on expected core burnup conditions. For this particular project, a Wet Annular Burnable Absorber (WABA) was considered for overall

assembly reactivity control due to its favorable operating characteristics. A WABA is a burnable poison insert, which is inserted into the control rod guide tubes of a fresh fuel assembly during its first cycle of operations (usually removed for the second and third cycles of operation), and consists of both poison rods and thimble plugs (thimble plugs are meant plug the holes of control rod guide tubes that do not have poison rods so as to control flow dynamics). Poison rods consists of an inner hollow annular region which allows water to flow through, which is then encircled by cladded poison material (see Figure 5)

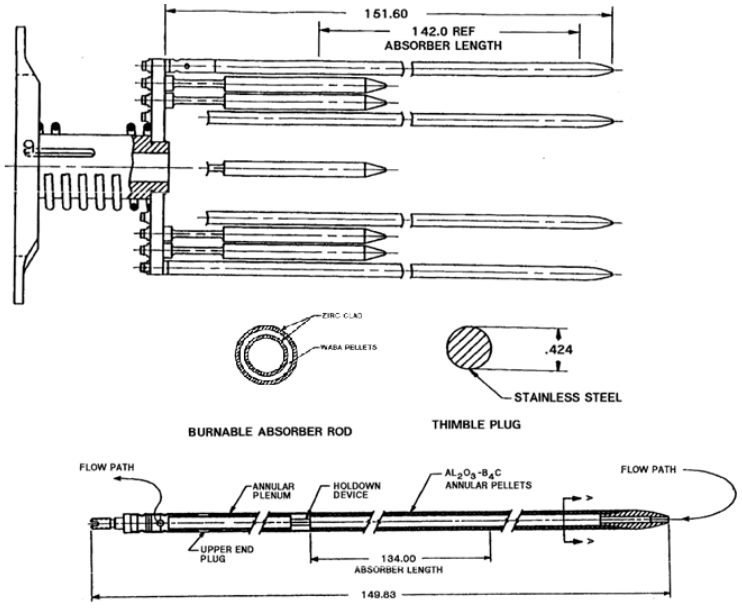

Figure 5 Typical WABA Design [14]

Though poison concentration in a WABA can be controlled by adjusting the amount of poison present in each poison rod, an alternative approach is to simply adjust the total number of poison rods in the WABA while leaving their concentrations the

same. Figure 6 illustrates the various WABA rod layouts that were considered in this project.

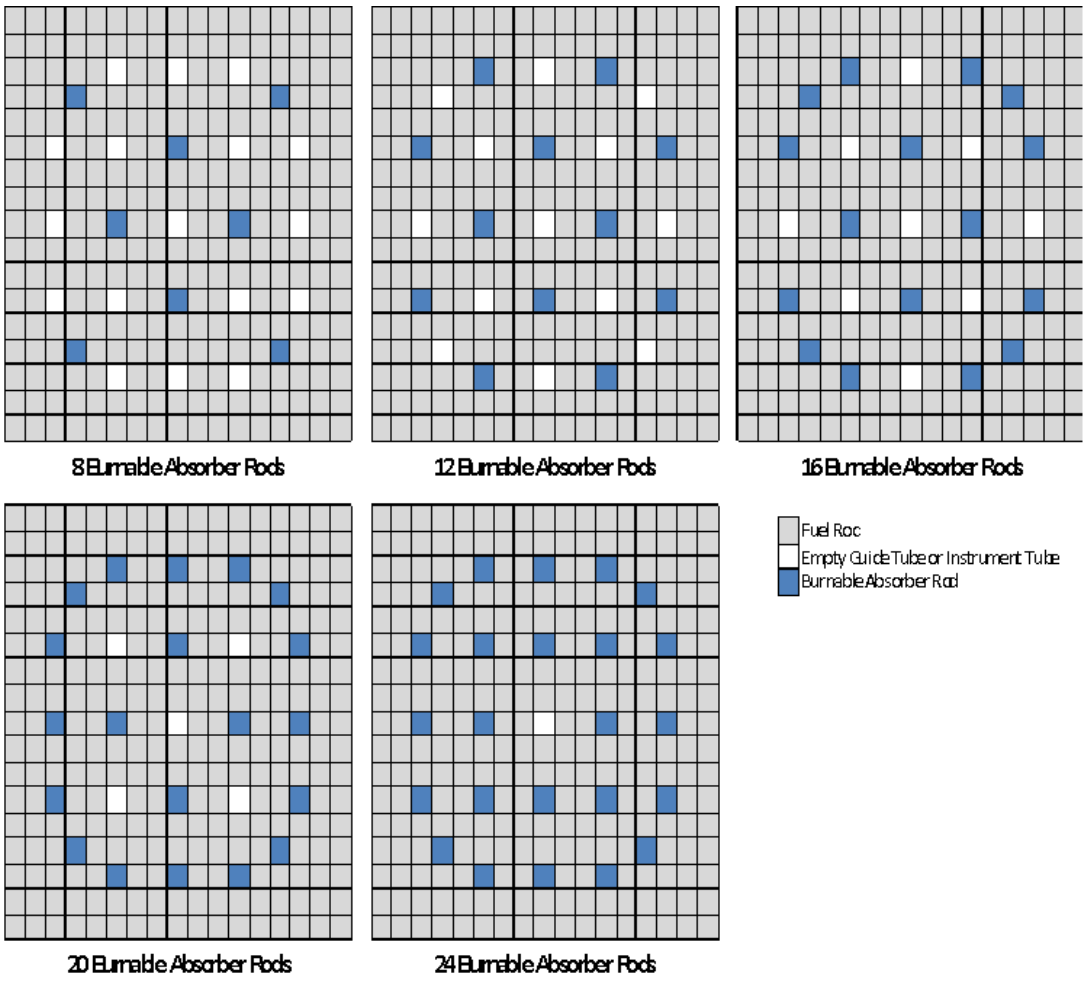

Figure 6 WABA Patterns Simulated [14]

In addition to using a WABA, Gd_2O_3 (a typical poison material) was added to the FCM rod, by means of dispersion throughout the pellet matrix material, for power peaking control of the FCM rods.

Table 1 / Figure 7 and Table 2 provide the important parameters used in this study for both assembly and core design (NOTE: Parameters do not necessarily correspond to a

particular real design being that all assemblies and cores, even among Westinghouse 4 PWRs and 17x17 assemblies, differ to some degree. As such, generic values were chosen which were believed to be representative [14,15,23]. Also the gap between the fuel pellet and clad, though existent, was ignored in these models).

Table 1 Assembly Pin Cell Dimensions (cm)

Cell Radius	Fuel Rod	Guide Tube	WABA
r1	0.412	0.562	0.2858
r2	0.476	0.613	0.3531
r3			0.4039
r4			0.4839
r5			0.562
r6			0.613

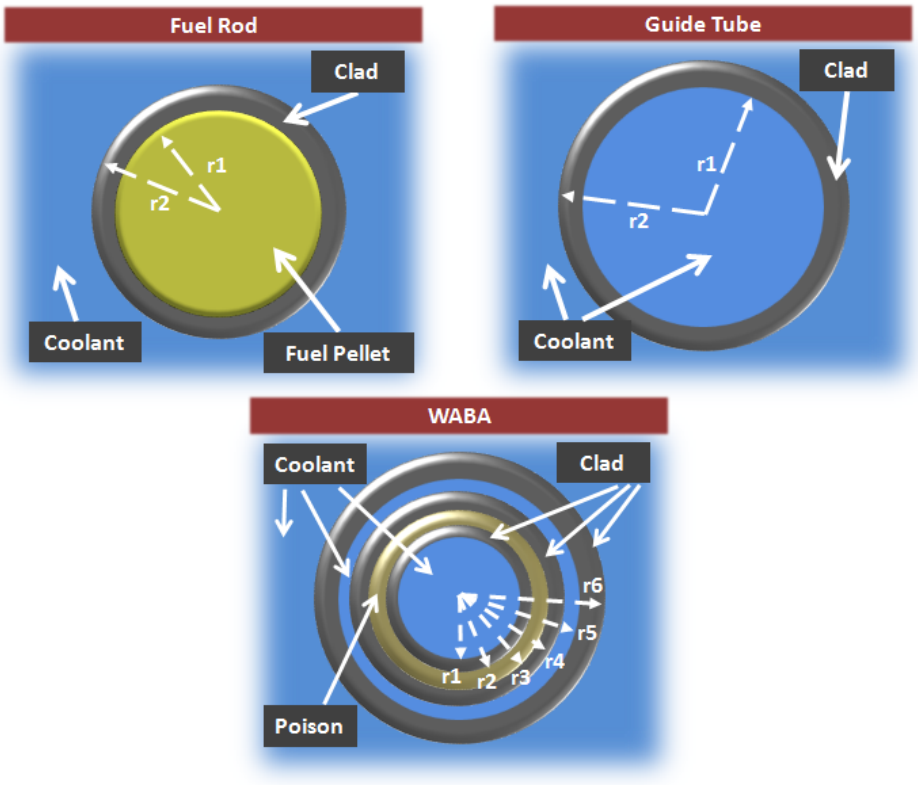

Figure 7 Assembly Pin Cell Geometries

Table 2 Assumed Core Design Parameters

Number of Fuel Assemblies	193
Power Level (MW_{th})	3411
Core Power Density (kW/L)	105
System Pressure, Nominal (psia)	2280
Nominal Coolant Inlet Temp (°F)	547.8
Core Average Fuel Temp (°F)	1160
Fuel Rods per Assembly	264
Control Rod Guide Tubes per Assembly	24
Instrument Tubes per Assembly	1
Coolant Mass Velocity ($lb_m/hr\text{-}ft^2$)	2.45
Active Fuel Length (in)	144
Assembly Pitch (in)	8.447
Pin Pitch (in)	0.497
Cladding Material	Zircaloy-4
WABA Poison Material	Al_2O_3-B_4C, 10% wt. B_4C
Target Cycle Length (Effective Full Power Days)	520

2. Methodology

In order to simulate the operating behaviors of fuel and core designs, the Oak Ridge National Laboratory's computer package SCALE along with the 3-D core simulator NESTLE were used. This chapter provides a brief description of the functionality of SCALE and NESTLE, as well as a discussion of techniques used for modeling the complex FCM fuel geometry.

2.1. SCALE

The Standardized Computer Analysis for Licensing Evaluation (SCALE) code package is a modeling and simulation suite for nuclear safety analysis. It provides a verified and validated tool set for criticality safety, reactor physics, radiation shielding, radioactive source term characterization, and sensitivity and uncertainty analysis. SCALE's code package consists of functional modules (modules which perform actual computations) and control modules (modules which manage data, formatting, and the running of functional modules to obtain a desired computations). The control modules TRITON and CSAS6, along with their associated functional modules, BONAMI, CENTRM, PMC, NEWT, ORIGEN, and KENO were used [16]. There are also coupling and formatting modules used by the control modules, but they will not be discussed in this report.

2.1.1. TRITON

TRITON is a multipurpose control module used in this project for performing lattice simulations of 2-D neutron transport calculations, relative power distribution calculations, and isotopic depletion. It was also used for generating few-group

homogenized cross-section data for use in NESTLE. Calculations are performed based on geometric configuration, composition content, expected average specific assembly powers, and output cross-section homogenization data provided by user input. TRITON begins by processing AMPX-generated multi-group cross-section data (in this case based on Evaluated Nuclear Data File Version VII data, ENDF/B-VII) by using CENTRM, BONAMI, and PMC to correct the AMPX cross-section data for resonance self-shielding and spectral effects. How it accounts for resonance self-shielding and spectral effects is based on user provided geometric input.

After processing the cross-section data, TRITON uses NEWT to perform 2-D discrete ordinates transport calculations and to generate few group (typically 2 group) cross-section data for nodal 3-D simulators (in this case NESTLE), based on the cross-section data processed with CENTRM, BONAMI, and PMC, and user provided input concerning geometry, transport calculation criteria, and few-group collapse parameters.

Finally, after the NEWT calculation, ORIGEN uses flux and power distribution results from NEWT along with the composition distribution, associated cross-section data, user designated depletion step size, and average specific assembly power to deplete the isotopes in the compositions. After this, the depleted compositions are re-assigned as the now current compositions at the beginning of a new time-step and the TRITON process is repeated for the designated number of depletion steps provided by the user to simulate the burning of an assembly and how it will behave over its entire life time.

NESTLE requires few group cross-section data for the entire range of anticipated fuel depletion at various operating conditions, which is generated in TRITON by using

branching feature. Using the branching feature, one can model at each depletion step instantaneous changes in fuel temperature, moderator temperature, moderator density, moderator boron concentration, and whether or not a control element (i.e. control rod) is present. This branching feature essentially runs multiple NEWT instances at each depletion step with each NEWT instance modeling a case with a given set of perturbations. The number of different branching cases and associate perturbations and their magnitudes are all designated by user input [17]. For generating the necessary data for NESTLE, one must designate average core operating conditions (average with respect to the entire core and entire operating cycle) on which TRITON will use as the basis for fuel depletion (in this report this case is referred to as the nominal case), and branches for the anticipated maximum and minimum conditions for each core parameter of interest (NOTE: NESTLE requires that for each branch, only one parameter be changed at a time while the rest remain at the average condition).

2.1.2. CSAS6

CSAS6 is a control module intended primarily for 3-D criticality safety calculations, but is only used in this project as a tool for benchmarking results to insure confidence in the functionality of the TRITON models that were used. CSAS6 uses KENO VI to perform reactivity calculations using a Monte Carlo based approach. User input is provided concerning compositions, geometries, and calculation parameters. Though KENO can be run using a multi-group structure similar to the methods used in TRITON (i.e. AMPX cross-section data processing), it was decided to use the continuous-energy cross-section model for performing these calculations due to its

expected superior accuracy. Continuous-energy models cannot currently be used in conjunction with depletion calculations, and so comparison may only be conducted for the initial conditions and not over the entire range of the fuel burn [18].

2.2. NESTLE

The Nodal Eigenvalue, Steady-state, Transient, Le core Evaluator (NESTLE) is a computer code that solves the few-group neutron diffusion equation by means of the Nodal Expansion Method (NEM) to perform a 3-D core simulation (NOTE: In this study NESTLE was used for 2-D core analysis to help simplify the modeling process). To create a model in NESTLE, a user must specify core geometry inputs, operating conditions or constraints, fuel exposure, desired solution method, and cross-section data. NESTLE is capable of solving power level and reactivity in a core based on user provided core conditions, or NESTLE can search for critical conditions based on power level, boron concentration, coolant inlet temperature, or control rod bank position. In the case of modeling PWR cores for feasible designs, the most appropriate solution method is to solve for critical conditions based on boron concentration. Cross-section data used in NESTLE is based on the few-group branching cross-section data generated from TRITON. NESTLE does not directly use the data generated from TRITON, but requires preprocessing of the data using a code called T2N to perform a Taylor's series expansion and polynomial fit of the TRITON data to create coefficients for use in NESTLE. NESTLE then uses these coefficients to effectively adjust cross-sections for changing conditions in the core.

For a given model, the few-group neutron diffusion equation is discretized using the NEM approach (in this case, where each node represents an individual fuel assembly), and is used to solve for the desired solution based the neutron leakage into and out of neighboring cells (i.e. boundary conditions) and conditions present within the cell and the designated solution method. Thermal-hydraulic conditions within a cell are modeled using a Homogenous Equilibrium Mixture model, I-135, X-135, and Sm-149 concentrations are modeled using the time-dependent depletion equations, and control rod position and boron concentrations are determined based on user designated input and solution method. Using this information, NESTLE can then solve for the desired solution in the cell whether it be a power level/reactivity solution or a critical condition solution. This process is repeated for all cells and thus simulates the operating conditions in the core [19].

2.3. Sources of Error in NESTLE Modeling

The NESTLE methodology uses burnup-dependent polynomial fits of macroscopic cross sections as a function of instantaneous perturbations (branches) on various core parameters, as those listed in Table 3, to perform cross section adjustments for actual nodal conditions (NOTE: though the control rod branch was read into the NESTLE input, it was never used due to modeling the core in an All-Rod-Out condition). At this time, however, NESTLE does not capture the effects on reactivity that result from altered isotopic depletion behavior from prolonged operation at perturbed (off reference) conditions, also known as history effects. Similarly, when changing from a cycle in which a burnable poison is present in a fuel assembly, to a cycle where the burnable

poison is removed, history effects are also lost due to the manner this problem was modeled in SCALE/TRITON. Lack of treatment of history effects in nodal simulations can have significant impacts on fuel cycle predictions, so this is potentially an important source of error that is not currently accounted for within the NESTLE code.

Table 3 List of Branching Cases and their Parameters

Branch Case	Moderator Density (g/cc)	Fuel Temp (K)	Moderator Temp (K)	Boron Conc. (ppm)	Control Present? (Y/N)
Base Case	0.723	900	580	630	N
Low Fuel Temp	0.723	550	580	630	N
Low Moderator Dens.	0.706	900	580	630	N
High Moderator Dens.	0.75	900	580	630	N
Low Boron Conc.	0.723	900	580	10	N
High Boron Conc.	0.723	900	580	1500	N
Control Rod Present	0.723	900	580	630	Y

Also, the act of using a few group energy structure (i.e. 2 groups) in NESTLE for modeling neutrons and cross-sections data results in an impact on the accuracy of the model as illustrated in Figure 8 and Figure 9.

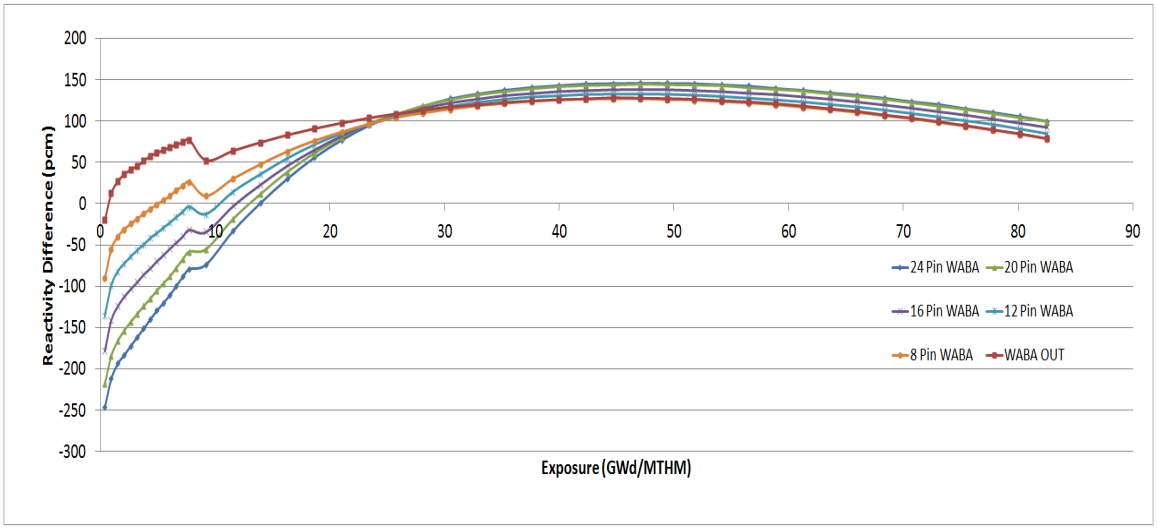

Figure 8 NESTLE - Multi-group TRITON Results Reactivity Difference

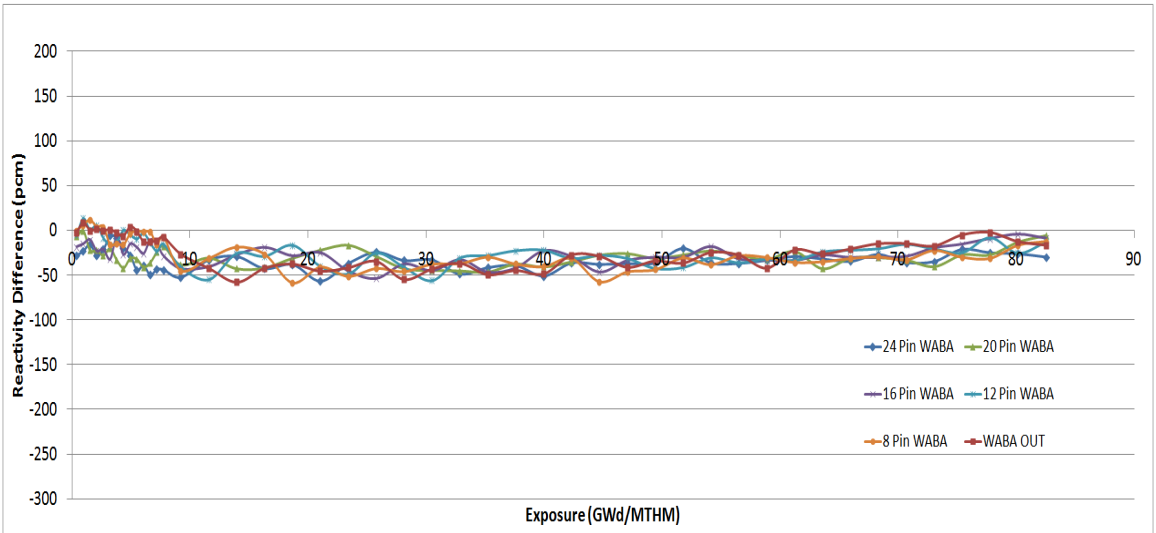

Figure 9 NESTLE - 2-group TRITON Results Reactivity Difference

In Figure 8, an infinite lattice case (identical to the model simulated in TRITON) was run in NESTLE and compared against the TRITON results that are based on a multi-group energy structure. In Figure 9 this same NESTLE case was compared against a manual calculation of the diffusion equation that was calculated using the few-group collapsed data extracted from TRITON and shows much better agreement [20]. In the comparison presented in Figure 8 the TRITON results are based on a multi-group energy structure (238 groups), where as in the Figure 9 comparison the manual calculation using the TRITON collapsed data is based on a few group energy structure (2 groups). These plots simply illustrates that simplification of the energy group structure will also have an impact on the NESTLE results such that they do not entirely match the original multi-group model used by TRITON. Since the core model itself will not be a reflective boundary condition case (i.e. the core will consist of all the same assembly, but with the assemblies not all having the same burnup or WABA design), it is expected that the error

induced by the group structure will , at worst, only be as large as the errors indicated by Figure 8 and Figure 9. For this analysis, these errors are not significant.

Finally, it should be noted that polynomial fits pertaining to the relationships of average fuel temperature vs. linear power density, effective heat transfer coefficient vs. fuel temperature, fuel surface temperature vs. linear power density, and fuel specific heat vs. temperature required by the NESTLE core simulator were chosen to be the same as fits used in the "Pin-Wise Loading Optimization and Lattice-to-Core Coupling for Isotopic Management in Light Water Reactors" doctoral thesis [21] due to lack of sufficient information for estimating these fits for this particular case. Being that the fuel lattice designs considered in this dissertation are not identical to those discussed below, some inaccuracy in modeling will be incurred, though not believed to be overly significant.

These above-noted anticipated sources of error in the current version of the NESTLE methodology and model are herein being provided for completeness. However, without having actual operational or experimental data at hand for an FCM fuel cycle it is simply impossible to quantify their true impact upon simulation predictions. Nevertheless, the errors introduced by these issues are believed to be adequately small for the sake of this scoping study.

2.4. Reactivity-equivalent Physical Transport

The model that is being analyzed for each individual FCM rod would be considered as complex multilayered geometries (i.e. the individual TRISO particles) dispersed throughout an additional multilayered geometry (i.e. the fuel Rod) illustrated in

Figure 10. TRISO particles are closely packed such that neutronic interactions between particles as well as the neutron slowing down within the fuel cannot be ignored. Also, fuel rods in the assembly are small enough that the heterogeneity of the fuel rod and interstitial moderator is important and the fuel particles cannot be considered to lie in an infinite medium. This geometric situation is often referred to as a Doubly-Heterogeneous geometry, which is treated in NEWT by performing a point-wise flux disadvantage factor calculation via CENTRM on the TRISO particles, using the calculation results to generate cell-weighted point-wise cross-sections for the homogenized fuel region in the fuel element, using these cross-sections in a second CENTRM run to calculate the flux distribution in the fuel rod, and finally using the flux distribution in PMC to generate the resonance self-shielding / spectral corrected cross-sections for modeling the fuel rod [16].

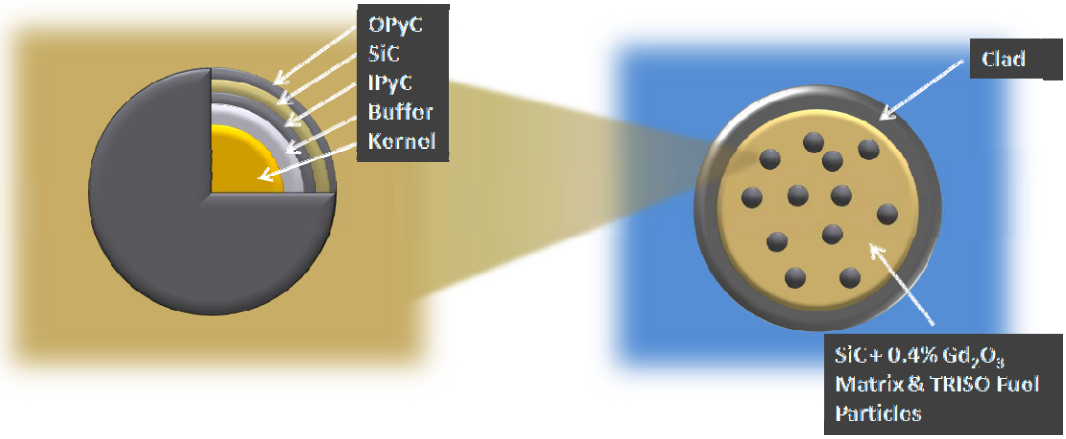

Figure 10 Illustration of 2-D Double Heterogeneous FCM fuel (Kernel Left / Rod Right)

Though TRITON is capable of modeling DH geometries, the DH modeling feature does not support the BRANCH function required for generating the cross-section data required for NESTLE nor does it support the ASSIGN function (a function for

simplifying the CENTRM processing of multiple similar geometries), which drastically improves the runtime of computations without significant loss in model accuracy (without which runtimes can be expected to be on the time scale of weeks for Non-Branching cases and longer for Branching cases, which is prohibitively long). To obtain an equivalent model without explicitly modeling a doubly heterogeneous structure, the Reactivity-Equivalent Physical Transform (RPT) method was used to model TRISO-based fuel rods [22]. In this methodology, the TRISO particles are artificially moved closer to the center of the pellet (within a limiting radius) providing an increased packing fraction, which in turn results in a change in reactivity. This is then counterbalanced by homogenizing the TRISO particles and matrix material within the new limiting radius resulting in an offsetting change in reactivity. The net effect is that the RPT method reproduces the reactivity of the system as calculated by a reference method (in this case the TRITON DH method). This process is illustrated in Figure 11.

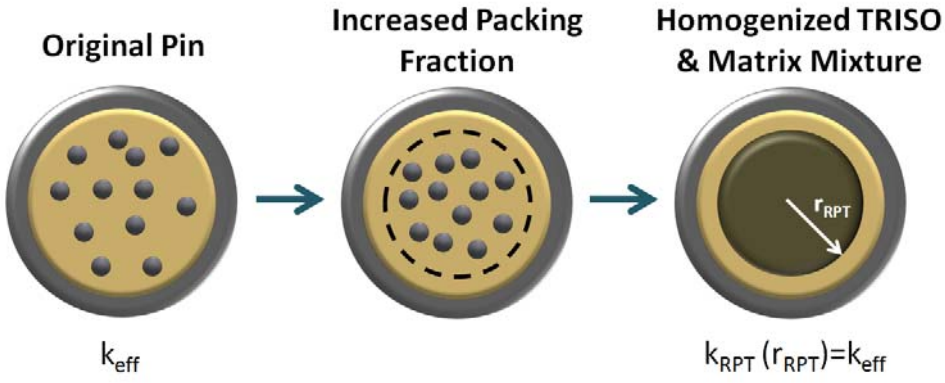

Figure 11 Illustration of RPT Methodology

By determining an appropriate equivalent radius, one can obtain a similar or equivalent reactivity behavior as the original doubly heterogeneous structure without

explicitly modeling it as such. The RPT approach enables the use of standard branching features available within SCALE/TRITON to generate the needed instantaneous branch calculations for the coupling to the 3D nodal simulator NESTLE.

2.4.1. RPT Single Rod Model Benchmark

To determine the RPT equivalent geometry for this particular model, an estimate was sought using a single rod model with reflective boundary conditions (i.e. modeling and infinitely large reactor made up of the one FCM rod type that is repeated and equally spaced in all directions). Though several FCM rod designs were attempted in pursuit of an most favorable design, the benchmarking that is discussed herein corresponds to the most optimal of those simulated. The actual specifics of this design will be discussed later in this manuscript. A reference Beginning-Of-Life (BOL) DH model was run using TRITON in addition to eight RPT models with various homogenized region radii. By plotting reactivity difference between the DH model and homogenized models with respect to the homogenized radii, an equivalent radius could be determined by which the reactivity difference was minimized. This procedure is illustrated in Figure 12.

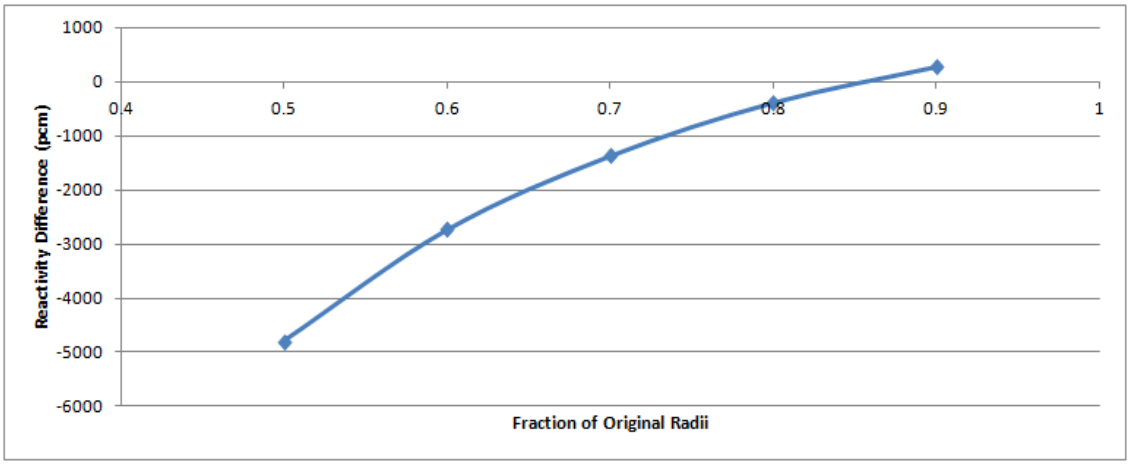

Figure 12 Difference Between the Reactivity Predicted by the RPT and DH Methods as a Function of the Fraction of Original Radius

For this case, the RPT equivalent radius was found to be 85.8% of the original fuel radius; 0.353 cm (estimated by performing a linear fit of the last two data points and solving for the intercept). To assess the correctness of this equivalent radius, a BOL comparison was made between the RPT model, the TRITON deterministic transport DH model, and a continuous energy KENO Monte Carlo DH model. In the case of the Monte Carlo model, the randomly distributed TRISO particles were modeled using a regular lattice for the sake of simplicity. All three models are illustrated in Figure 13 with the resulting comparison in BOL reactivity differences tabulated in Table 4 (NOTE: The TRITON model [far left] appears homogenized, but it is in fact modeling a DH geometry).

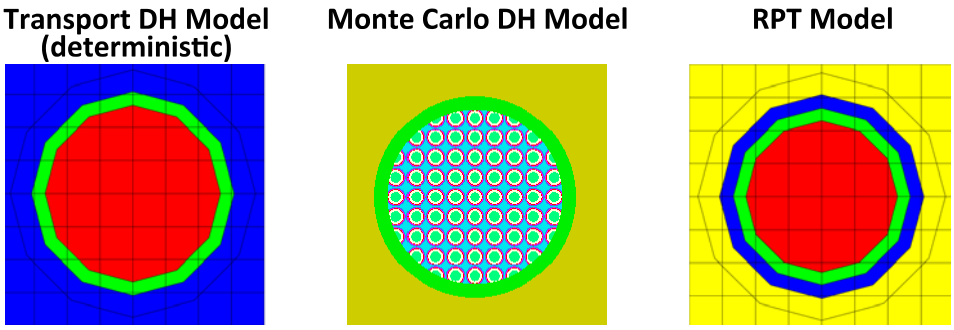

Figure 13 Single Rod Models

Table 4 Reactivity Difference Between Modeling Methods at BOL

Transport Double-Het k_{eff}	**Monte Carlo Double-Het k_{eff}**	**Transport RPT k_{eff}**
1.173519	1.173589	1.173942
RPT -Transport DH Reactivity Difference (pcm)	**RPT -Monte Carlo DH Reactivity Difference (pcm)**	**Transport DH -Monte Carlo DH Reactivity Difference (pcm)**
42.4	35.3	-7.0

It is believed from comparing the BOL reactivity differences that the RPT method very nearly estimates the same reactivity as the deterministic DH model, and also compares well with the Monte Carlo DH model. To further evaluate the accuracy of this methodology, a comparison between an RPT depletion model and a TRITON transport-based DH depletion model was performed with respect to exposure (NOTE: Exposure is a measure of energy produced per unit of heavy metal mass in the fuel. In this case giga watts days per metric ton of heavy metal or GWd/MTHM), as seen in Figure 14. The continuous energy KENO modeling does not currently have depletion capability and therefore a comparison with Monte Carlo depletion results was not possible.

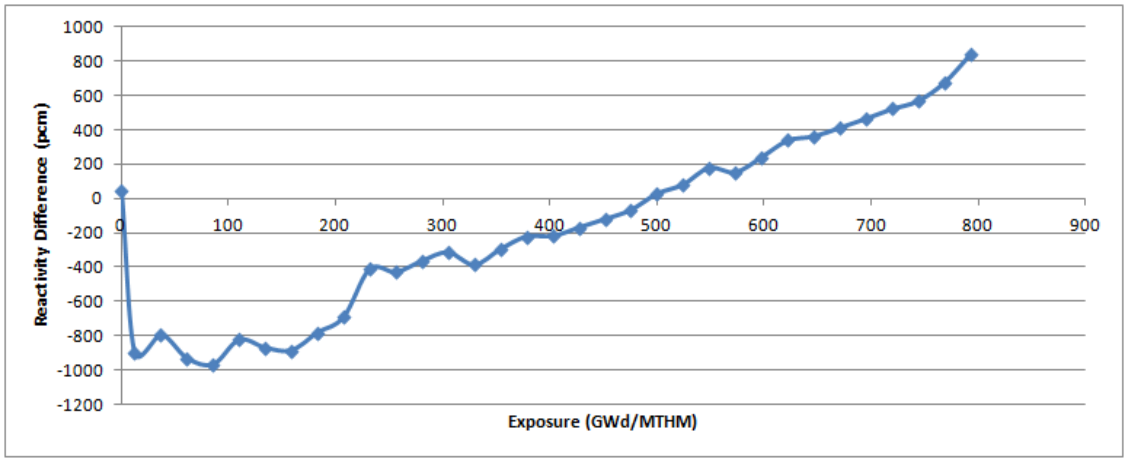

Figure 14 RPT - TRITON DH Single Rod Reactivity Differences vs. Exposure

Based on the results shown in Figure 14, the agreement between RPT and TRITON DH diverges considerably post BOL. It quickly jumps to nearly -1% and then steadily changes to about +1% near 800 GWd/MTHM. This disagreement behavior is believed to be the result of the RPT method not accounting for changing flux spectral effects caused by changing fuel composition from depletion (NOTE: it may be possible to improve this error by basing the RPT equivalent radius on a later time step, but this study will use BOL as the basis time step). Although this large disagreement as a function of exposure is observed and herein documented, the overall effect upon the calculations performed is not expected to be nearly as significant because (1) only a fraction of the fuel rods in each bundle are FCM designs (i.e. the plot provided in Figure 14 is the equivalent of an assembly entirely composed of FCM rods, so any assembly design not entirely composed of FCM rods will have a smaller error from FCM RPT modeling), and (2) this discrepancy swaps sign as a function of exposure, thus potentially providing some cancellation of errors between low and high burnup FCM rods. Regardless, until new

SCALE features under development at ORNL can address double-het and lattice physics branches simultaneously, the use of RPT for this study is necessary to be able to develop full core nodal models using TRITON and NESTLE.

2.4.2. RPT Quarter Lattice Model Benchmark

Using the RPT equivalent model for the FCM fuel rods, modeling was conducted on the quarter lattice level (with reflective boundary conditions to simulate an infinitely sized core made up of an identical lattices repeated in all directions). Though several lattice designs were attempted in pursuit of a most favorable design, the benchmarking that is discussed herein corresponds to the most optimal of those simulated. The actual specifics of this design and the lattice performance results will be discussed later in this manuscript. This section will focus only on comparative benchmarking of RPT lattice model to demonstrate confidence in the accuracy of the results.

In order to demonstrate confidence of using RPT with the various poison loadings in the most optimized lattice design, benchmarks were performed for every WABA rod layout (along with the case in which no WABA was used). Reactivity, relative rod power, and isotopic mass estimates were deemed the most important values to compare, and these results are shown in Figure 15 thru Figure 26 as well as Table 5 and Table 6 (NOTE: KENO was only used for benchmarking k-eff at BOL). In order to benchmark the RPT branching cases against the explicit Transport DH model, models were manually created for three time steps for each perturbation of interest that mostly covers the expected assembly life time. Only a select number of time steps were chosen due to the inherent difficulty of creating these models and the computing time required to do so.

These select steps are meant to provide confidence that the overall trends do not change greatly with respect to changes in the operating conditions.

Table 5 BOL KENO Model Comparison Reactivity Difference (pcm)

	24 Pin WABA	**20 Pin WABA**	**16 Pin WABA**	**12 Pin WABA**	**8 Pin WABA**	**WABA OUT**
RPT-KENO DH	-99.181	-127.166	-159.582	-176.944	-187.398	-267.474
TRANSPORT DH-KENO DH	147.628	122.787	97.871	88.236	87.067	13.275

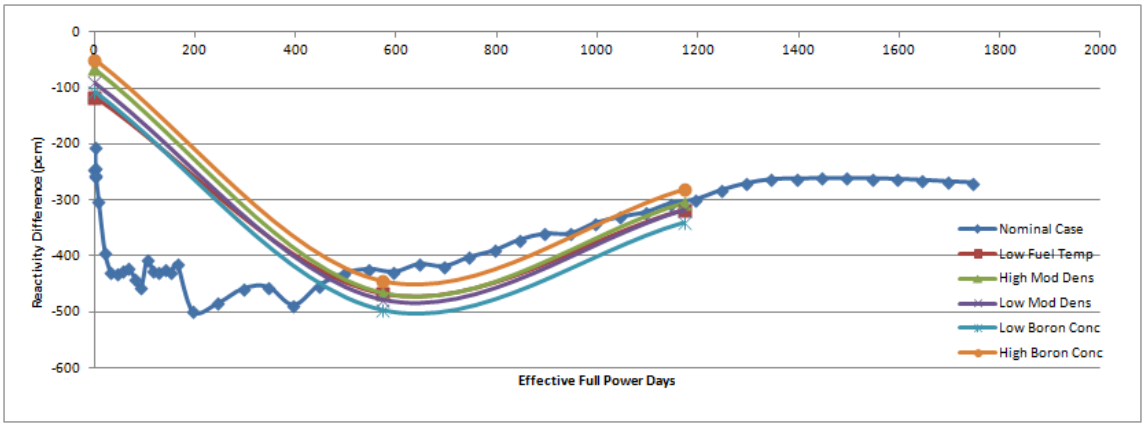

Figure 15 WABA 24 Pin RPT - Transport DH Lattice Reactivity Difference

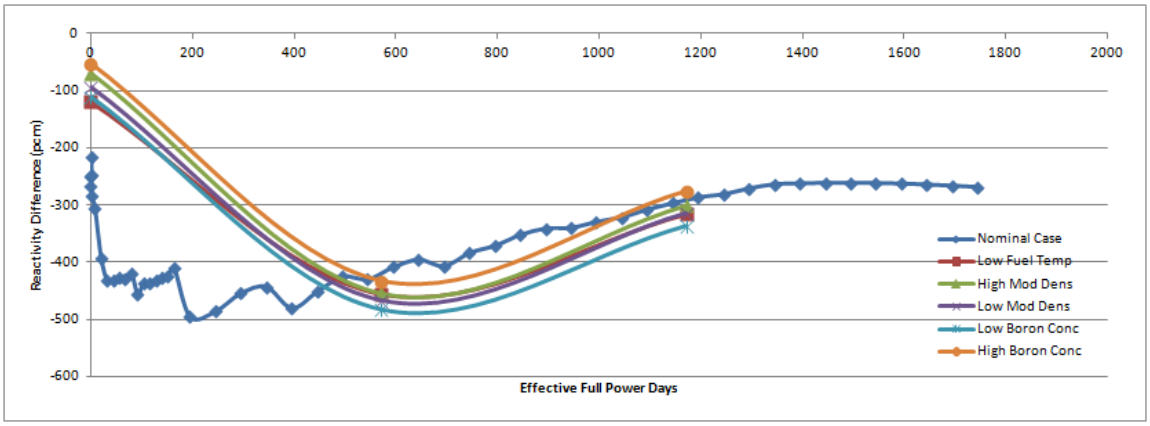

Figure 16 WABA 20 Pin RPT - Transport DH Lattice Reactivity Difference

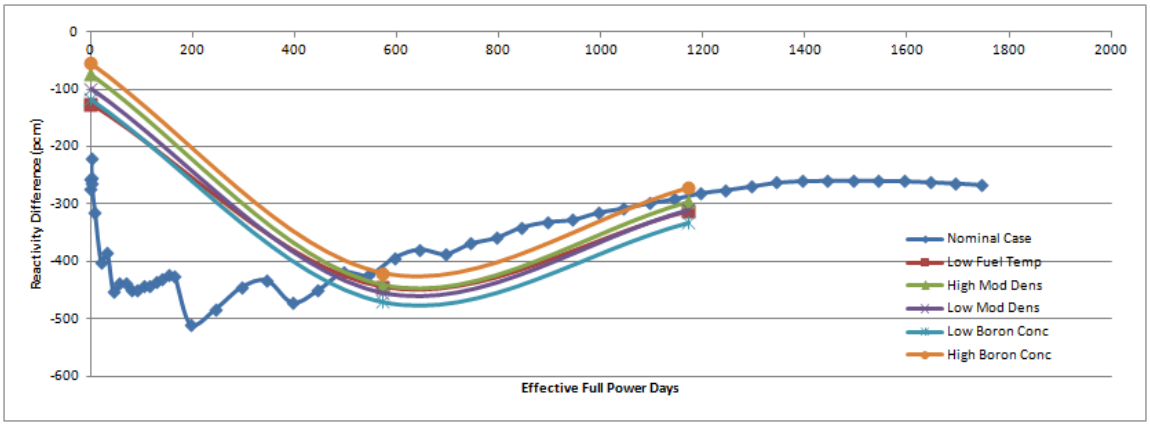

Figure 17 WABA 16 Pin RPT - Transport DH Lattice Reactivity Difference

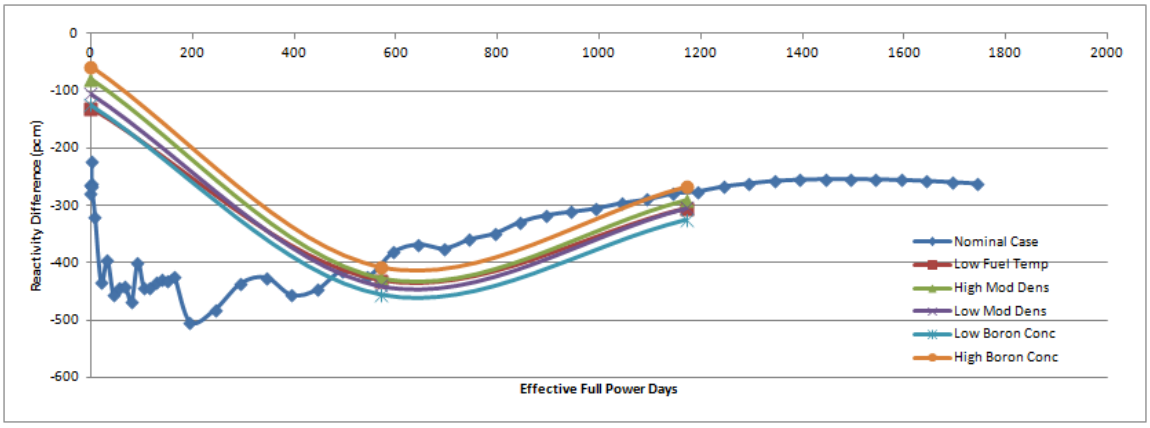

Figure 18 WABA 12 Pin RPT - Transport DH Lattice Reactivity Difference

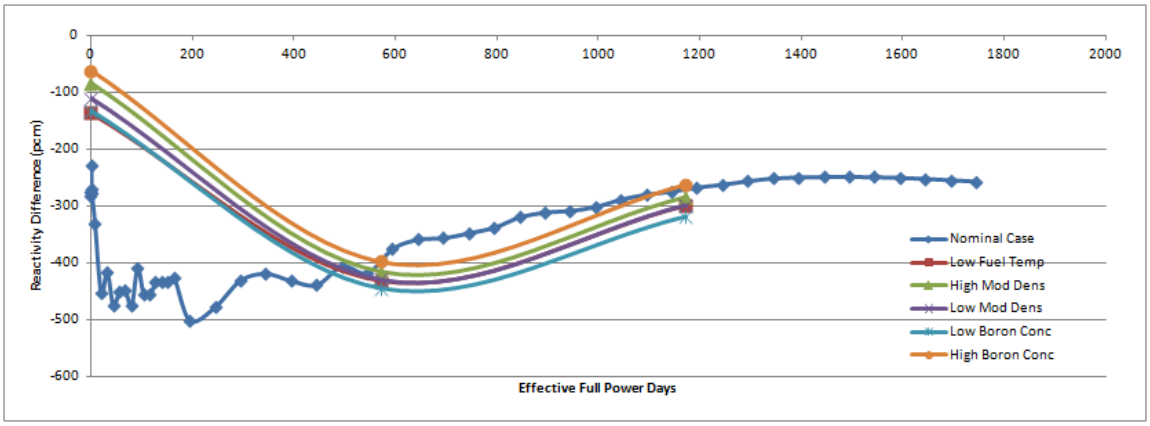

Figure 19 WABA 8 Pin RPT - Transport DH Lattice Reactivity Difference

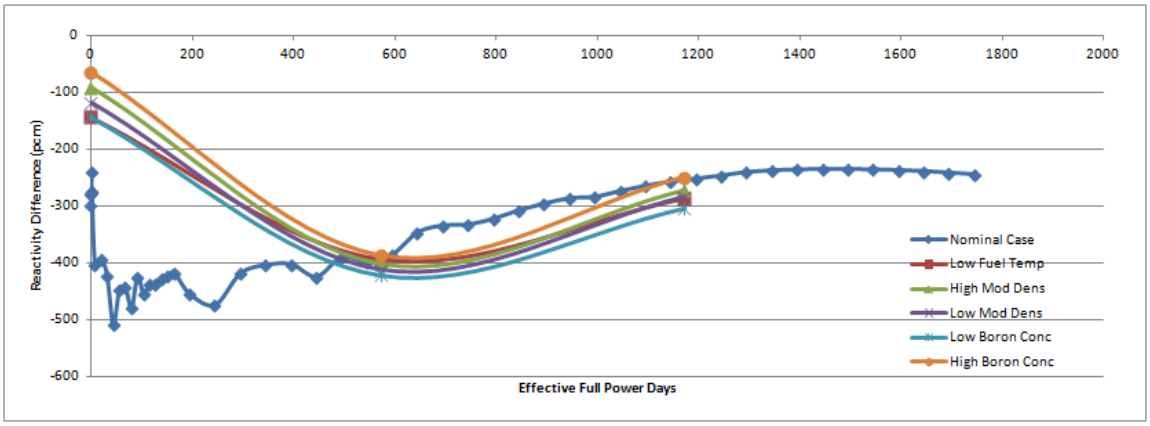

Figure 20 WABA Out RPT - Transport DH Lattice Reactivity Difference

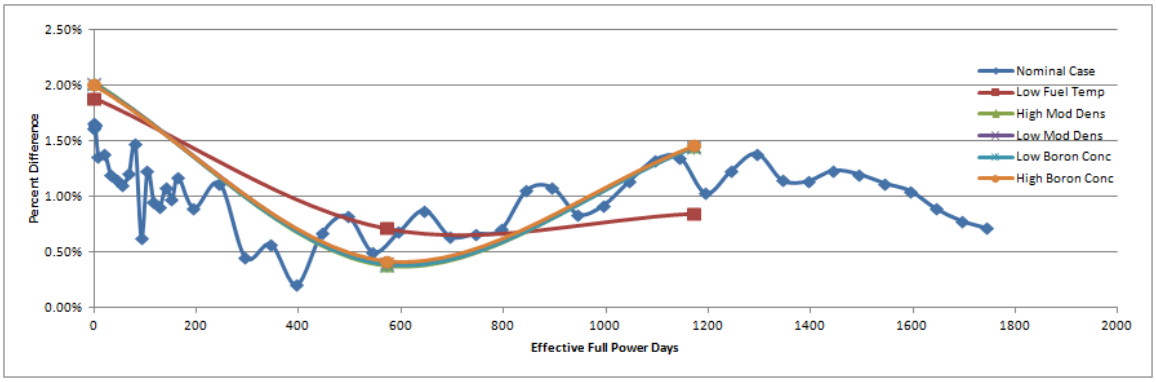

Figure 21 WABA 24 Pin RPT - Transport DH Lattice Rod Power Maximum Percent Difference

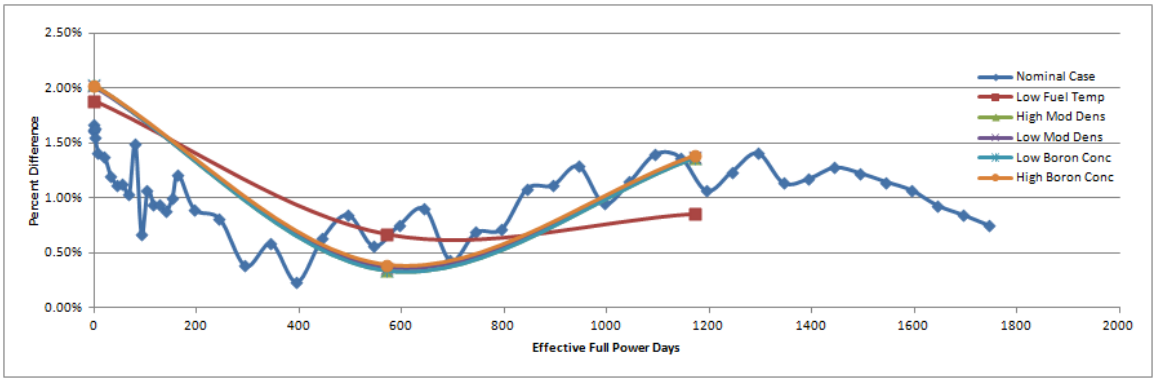

Figure 22 WABA 20 Pin RPT - Transport DH Lattice Rod Power Maximum Percent Difference

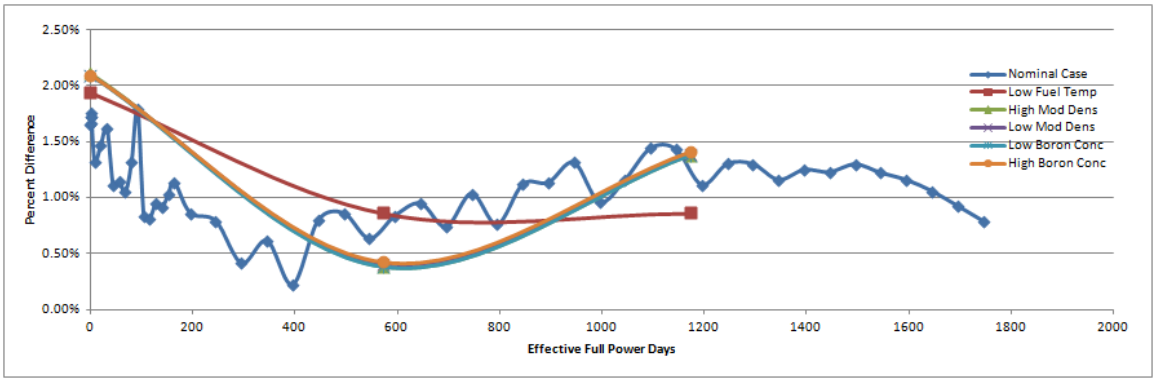

Figure 23 WABA 16 Pin RPT - Transport DH Lattice Rod Power Maximum Percent Difference

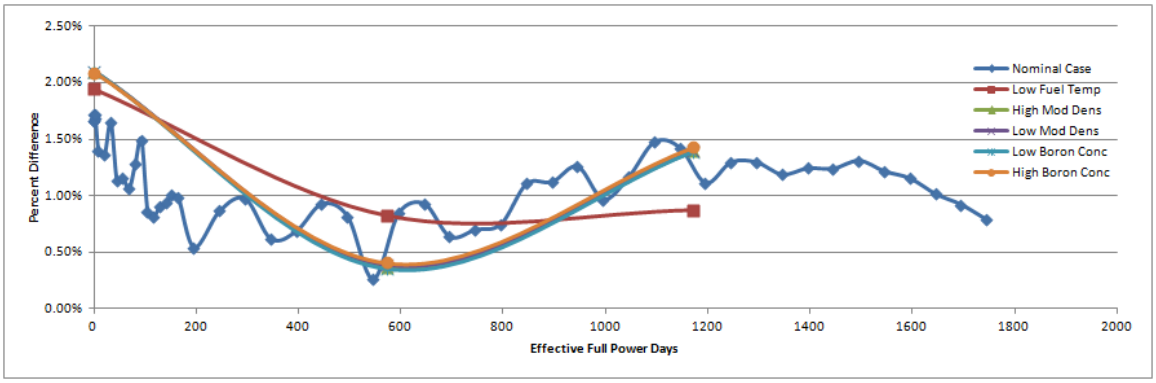

Figure 24 WABA 12 Pin RPT - Transport DH Lattice Rod Power Maximum Percent Difference

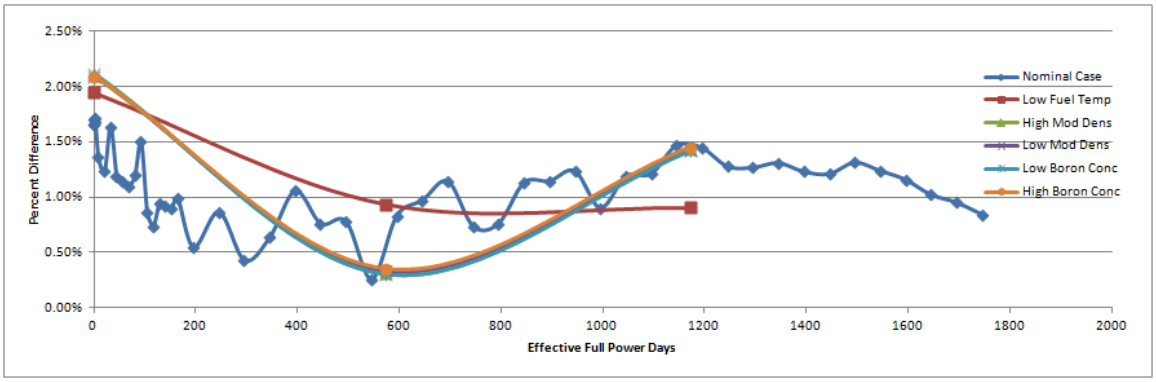

Figure 25 WABA 8 Pin RPT - Transport DH Lattice Rod Power Maximum Percent Difference

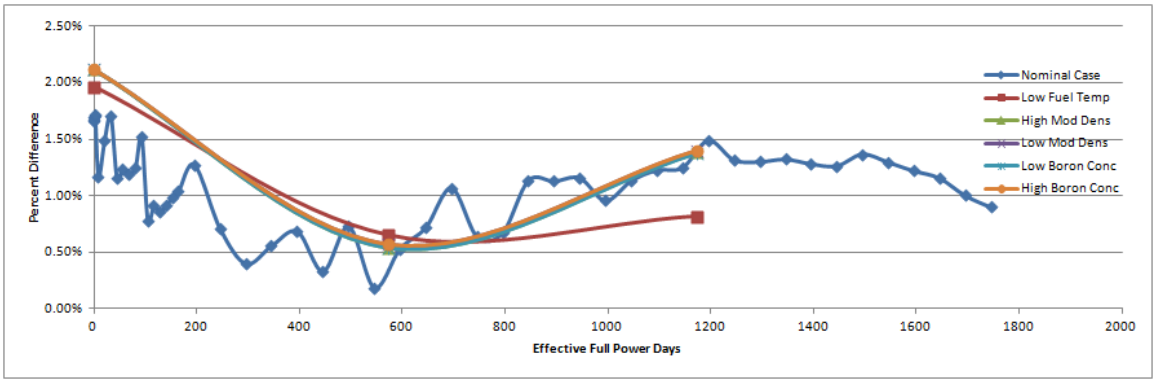

Figure 26 WABA Out RPT - Transport DH Lattice Rod Power Maximum Percent Difference

Table 6 RPT - Transport DH End of Life Isotopic Mass Percent Difference

	WABA 24 Pin	**WABA 20 Pin**	**WABA 16 Pin**	**WABA 12 Pin**	**WABA 8 Pin**	**WABA OUT**
nuclide	RPT - Transport DH % Difference					
u235	0.44%	0.40%	0.38%	0.36%	0.36%	0.37%
u238	0.44%	0.40%	0.38%	0.36%	0.36%	0.37%
np237	-0.14%	-0.09%	-0.09%	-0.18%	-0.18%	-0.09%
pu238	0.57%	0.62%	0.62%	0.57%	0.58%	0.58%
pu239	-0.08%	-0.12%	-0.13%	-0.15%	-0.17%	-0.18%
pu240	-1.34%	-1.35%	-1.35%	-1.37%	-1.38%	-1.36%
pu241	-0.06%	-0.07%	-0.07%	-0.07%	-0.07%	-0.07%
pu242	-1.10%	-1.09%	-1.07%	-1.07%	-1.07%	-1.02%
cs-137	-0.06%	-0.04%	-0.04%	-0.04%	-0.04%	-0.04%
ba-137	-0.08%	-0.03%	-0.05%	-0.05%	-0.03%	-0.05%
sr-90	-0.08%	-0.07%	-0.07%	-0.07%	-0.07%	-0.06%
y-90	-0.21%	-0.21%	-0.19%	-0.19%	-0.19%	-0.19%
pr-144	-0.05%	-0.05%	0.00%	-0.02%	0.00%	-0.02%
am-241	0.17%	0.19%	0.15%	0.10%	0.15%	0.13%
zr-93	-0.07%	-0.07%	-0.07%	-0.05%	-0.07%	-0.07%
nb-93	-0.13%	-0.13%	-0.13%	-0.13%	-0.13%	-0.10%
cs-135	0.42%	0.41%	0.41%	0.41%	0.40%	0.40%
i-129	-0.06%	-0.06%	-0.06%	-0.07%	-0.06%	-0.06%
tc-99	-0.13%	-0.09%	-0.09%	-0.13%	-0.09%	-0.13%
np/pu Total	-0.51%	-0.52%	-0.53%	-0.55%	-0.56%	-0.55%
WasteTotal	-0.10%	-0.12%	-0.13%	-0.15%	-0.15%	-0.15%

In the reactivity curves, it can be seen that there is a prompt increase in the magnitude of difference between the RPT and transport DH models at BOL to approximately 500 pcm, which then gradually decreases to a difference between 200 and 300 pcm as the fuel depletes. Also, looking at the BOL comparison against the Monte Carlo DH lattice model that there is fairly good agreement between it and the RPT model. This difference is less than what was seen in the case of the single rod models because not all rods in the assembly are FCM rods (i.e. some are typical UO_2 rods). Looking at the 3 data points for each branch, it is believe to be reasonable to conclude that the branching cases will behave very similarly to the nominal case.

The maximum percent differences in the relative rod powers shown in the figures indicate good agreement between the RPT and transport DH models, despite the somewhat significant reactivity differences. The maximum percent differences appears to mainly fluctuate between 1.7% and 0.00% for the nominal, and between 2.1% and 0.00% for the worst case branch.

Isotopic concentrations also appear to not be greatly affected by the reactivity differences between the RPT and transport DH model. The larges magnitude of percent difference appears to be for the Pu-240 isotope in the 8 Pin WABA model, with a value of -1.38%.

Though the reactivity differences can be somewhat significant when comparing RPT with the other models, one can see that the pin power and isotopic results are not greatly affected by this difference in reactivity (as far as the RPT and Transport DH models are concerned). It is then believed that the RPT methodology is adequately

accurate for these scoping studies and so can be used for quarter lattice modeling and generating two group cross section libraries for the full core analysis.

2.5. Equilibrium Core Design Methodology

This study aimed to show that a viable core design could be achieved by assembling an equilibrium core design or equilibrium series of core designs. At equilibrium, the core loading or a series of core loadings may continuously be repeated indefinitely without changing core operational behavior. This is accomplished by taking an initial guess of the assembly burnup distributions, running NESTLE using a critical soluble boron parameter search to simulate a full cycle of operation, shuffling the assemblies at the end of each cycle using a fixed shuffle plan (or series of fixed shuffle plans) and re-running NESTLE. This process is repeated until eventually the assembly burnup distributions no longer change between cycles or between shuffle plans, which defines the achievement of an equilibrium core that can be employed to assess the various neutronics parameters and attributes of interest.

3. Results and Discussion

Though the process of finding appropriate fuel and core designs itself was iterative in nature and a large variety of different assembly types and core designs was simulated, only what is considered to be the best results to date based on relative power, reactivity, and isotopic behaviors are discussed below.

3.1. Lattice Modeling

Typical PWR fuel assemblies are designed with an initial enrichment of nearly 4.5% [23], and so the optimal lattice design was considered to be a design in which lattice behavior is similar to a lattice in which every fuel rod consists of UO_2 that is 4.5% enriched. Optimal FCM rod designs consisted of TRISO particles and matrix material with compositions and parameters provided in Table 7 and Table 8. The TRISO fuel kernel compositions were based on expected isotope concentrations from the discharge fuel that are to be recycled along with using a 20 mole% SiC getter mixture to account for the expected burnup of fuel material of the course of the assembly life (NOTE: the Transuranic isotopic concentrations are representative of discharge UO_2 fuel)[12,24,25]. The matrix composition is based on typical fabricated compositions mixed with Gd_2O_3 to an amount of 0.4 wt% to suppress power peaking in the FCM rods during the early assembly life caused by the Plutonium having a greater thermal fission cross-section (NOTE: the matrix isotopic concentrations for Si, Al, C, and Y are representative of typical fabrication weight percentages)[10].

Table 7 FCM Fuel Compositions

Material	Element	Number Density (atoms/b-cm)
Fuel Kernel	c	5.42E-03
	si-28	5.00-03
	si-29	2.53E-04
	si-30	1.8E-04
	o-16	3.49E-02
	u-235	3.03E-07
	u-238	4.30E-05
	np-237	1.08E-03
	pu-238	6.53E-04
	pu-239	1.26E-02
	pu-240	4.75E-03
	pu-241	1.11E-03
	pu-242	1.42E-03
Buffer Layer	c- graphite	5.02E-02
IPyC Layer	c - graphite	9.54E-02
SiC Layer	SiC	4.81E-02
OPyC Layer	c - graphite	9.38E-02
Matrix	o-16	2.54E-03
	c	4.61E-02
	si-28	4.25E-02
	si-29	2.15E-03
	si-30	1.43E-03
	Y-89	2.91E-04
	Al-27	1.36E-03
	gd-154	9.52E-07
	gd-155	6.46E-06
	gd-156	8.94E-06
	gd-157	6.83E-06
	gd-158	1.08E-05
	gd-160	9.55E-06

Table 8 FCM TRISO Parameters

Kernel Radius (cm)	0.025
Buffer Layer Thickness (cm)	0.035
IPyC Layer Thickness (cm)	0.0385
SiC Layer Thickness (cm)	0.042
OPyC Layer Thickness (cm)	0.046
Packing Fraction	50%

Lattice optimization was conducted using a combination fuel composition and rod location iteration, along with consideration of the previously proposed CORAIL MOX design [2]. The currently most optimized lattice design consists of 60 FCM fuel rods loaded on the periphery of the fuel assembly, with the remaining fuel consisting of 4.5% enriched UO_2 fuel rods, as shown in Figure 27. This rod layout (i.e. peripheral loading of FCM rods) was chosen due to its ability to equalize the distribution of rod power by forcing the highly reactive FCM rods to "compete" with FCM rods from neighboring assemblies and thus keep them from absorbing too much of the thermal neutron flux and experiencing too great of power peaking. Interior FCM rod placement designs were analyzed, but were found to have unfavorable power distributions due to the Plutonium rods out absorbing the UO_2 rods, in terms of neutrons, resulting in a suppression of power in the UO_2 rod and an unacceptably high power peaking in the FCM rods. Similar Plutonium rod layouts to the one chosen as the most optimal for this study were used with the CORAIL MOX design as well as other recent FCM PWR fuel studies [2,12].

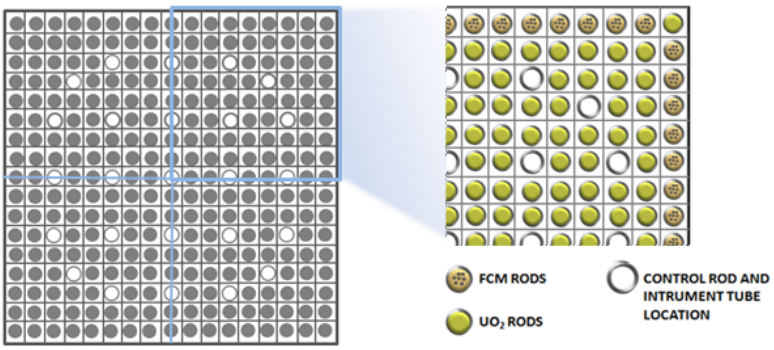

Figure 27 Quarter Lattice Layout with Periphery FCM Rods

Figure 28 thru Figure 33 provide a reactivity comparison of the TRITON 2-D results between a conventional 4.5% enriched UO_2 assembly and the proposed FCM lattice design with the various WABA poison loadings. As can be seen, the general behaviors are very similar with the largest differences occurring at BOL and the estimated assembly End-of-Life (EOL) of 1500 Effective Full Power Days (EFPD). The worst case (i.e. the WABA OUT lattice) BOL reactivity difference quickly drops from 6000 pcm to 4000 pcm in the first two days. This difference eventually becomes less than 1000 pcm after the first 44 days, followed by the FCM lattice showing greater reactivity than the UO_2 for a period of time (greatest difference of ~500 pcm for the 24 Pin WABA case). Finally, the FCM lattice reactivity eventually drops below that of the UO_2 assembly with the difference increasing all the way till EOL (maximum difference of ~3000 pcm). These differences, though not excessive, impact assembly power distribution on the core level and could potentially create challenges for core design. The lowered EOL reactivity could possibly limit the number of twice burned assemblies that can be used in a core design such that the desired cycle length is still reached. It may also create issues with assembly power sharing (i.e. assembly power peaking) being that fresh and once burned assemblies will have to produce greater amounts of the core's power in order to compensate for the lower amount of power produced in the twice burned assemblies. Final assessment of the acceptability of these reactivity behavior difference may only be determined through core design (i.e. if a core using this FCM fuel can be designed with acceptable results, then the lattice design will be acceptable).

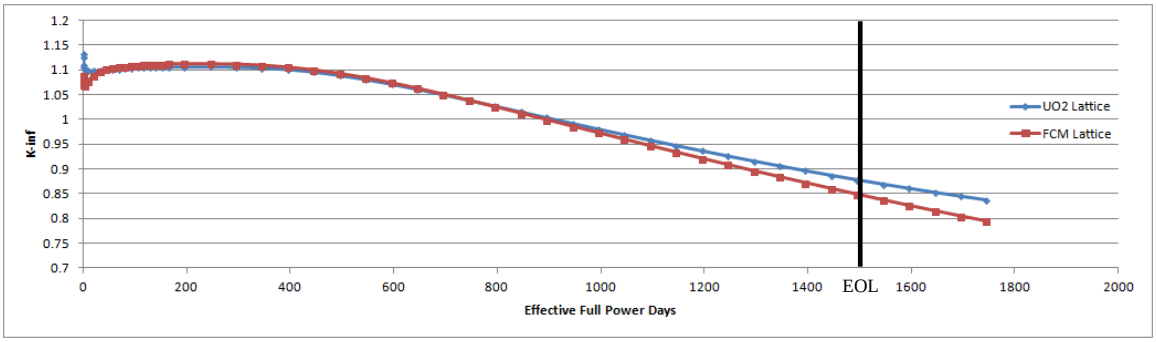

Figure 28 WABA 24 Pin Lattice K-inf Comparison of FCM and UO_2 Fuel

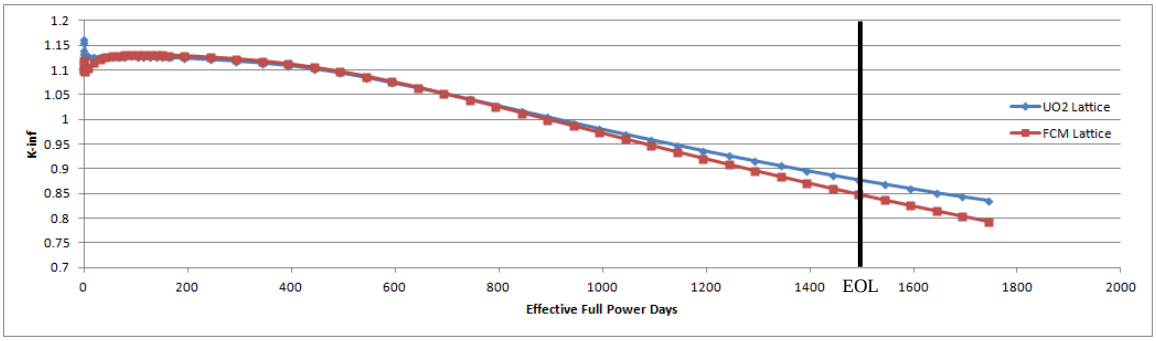

Figure 29 WABA 20 Pin Lattice K-inf Comparison of FCM and UO_2 Fuel

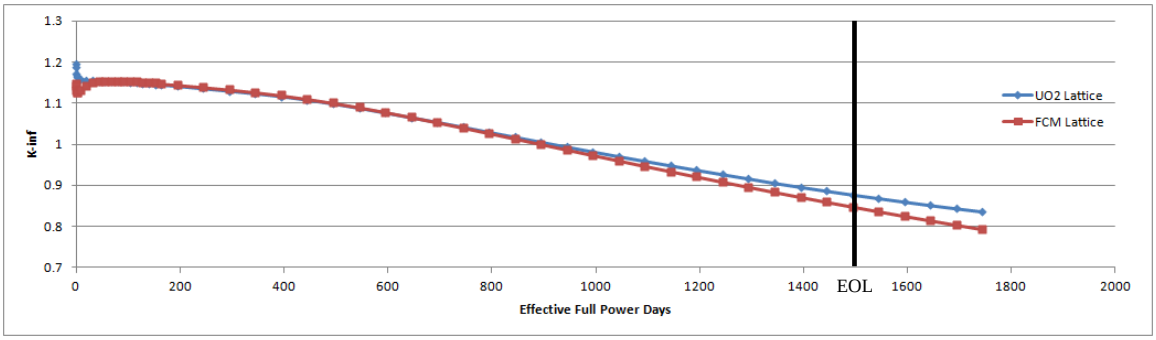

Figure 30 WABA 16 Pin Lattice K-inf Comparison of FCM and UO_2 Fuel

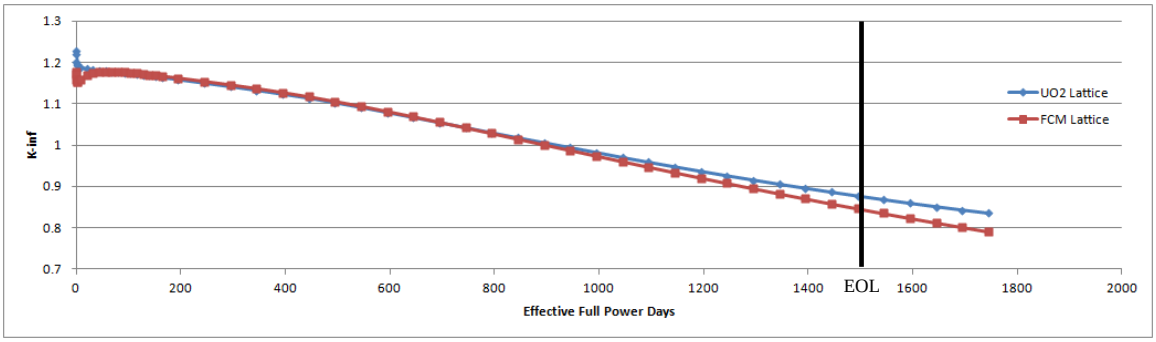

Figure 31 WABA 12 Pin Lattice K-inf Comparison of FCM and UO_2 Fuel

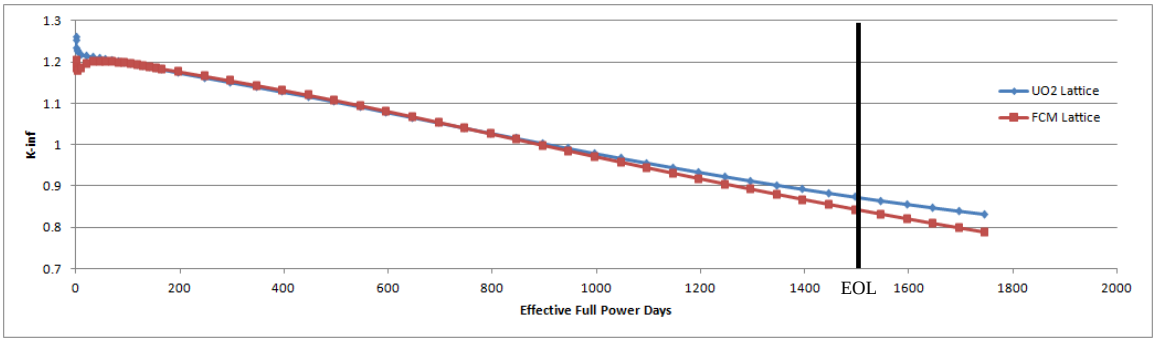

Figure 32 WABA 8 Pin Lattice K-inf Comparison of FCM and UO_2 Fuel

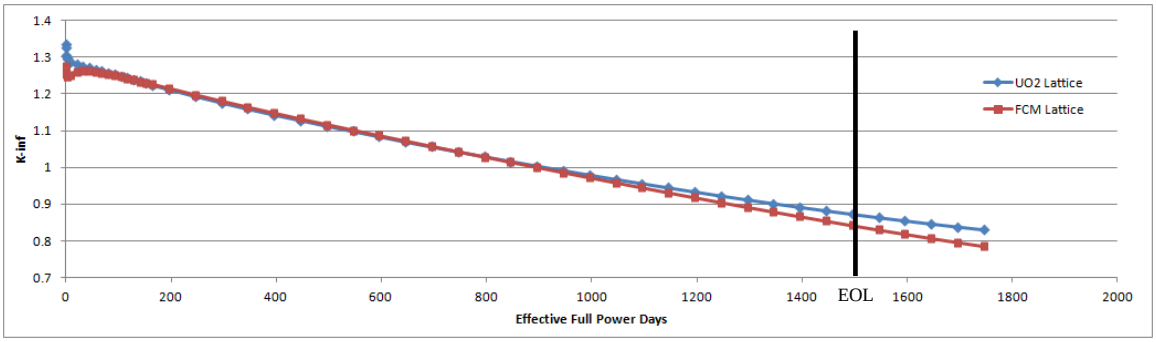

Figure 33 WABA Out Lattice K-inf Comparison of FCM and UO_2 Fuel

When optimizing the lattice design, it was desired to have a maximum relative rod power less than 1.2, but this was not obtained. Figure 34 thru Figure 39 illustrates the maximum relative rod power behaviors for both the FCM fuel rods and UO_2 fuel rods in the FCM assembly. For the worst case (i.e. 24 pin WABA) the maximum UO_2 relative rod power is shown to be about 1.179 at BOL and the maximum FCM rod power to be about 1.21 shortly after BOL, are similar results as those seen in the FCM PWR lattice research conducted by KAERI [12]. For the UO_2 rods, the relative power peaking first dips and then gradually increases over the assembly lifetime up to approximately 1.28 at EOL, but this is not of too significant being that by the time this exposure is achieved, the assembly is expected to reside in a lower power region of the core. As such, though the relative rod power may be high, overall assembly power is low, and so the maximum power produced by the rod should not be of concern. It is not known at this time whether FCM rods may have a higher threshold for power peaking due to their improved thermal conductivity. However, the purpose of this evaluation is to simply confirm that the power peaking determined falls within a reasonable range, similar to those for the simulated UO_2 lattices (~1.14) as well as being somewhat consistent with results observed by others.

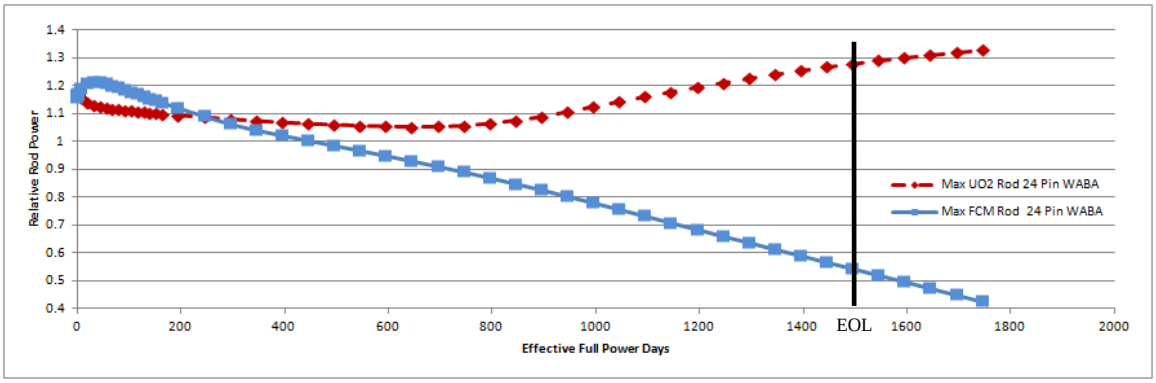

Figure 34 WABA 24 Pin FCM Lattice Max Rod Power

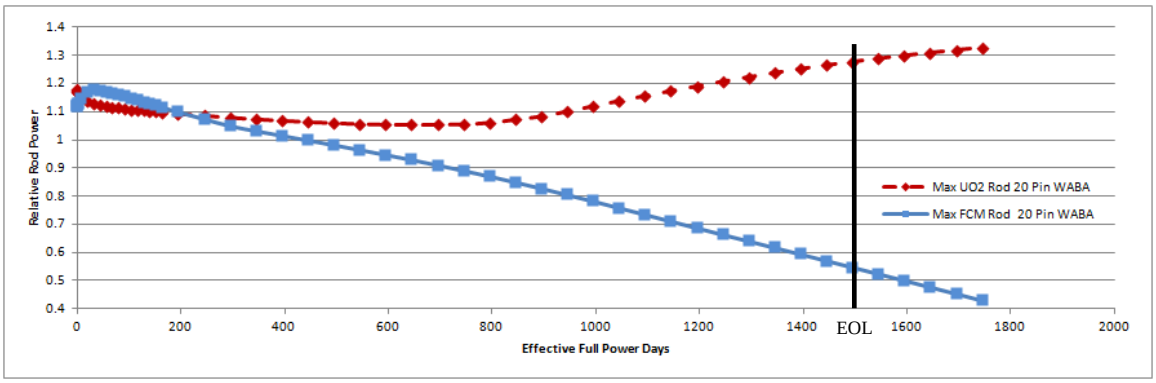

Figure 35 WABA 20 Pin FCM Lattice Max Rod Power

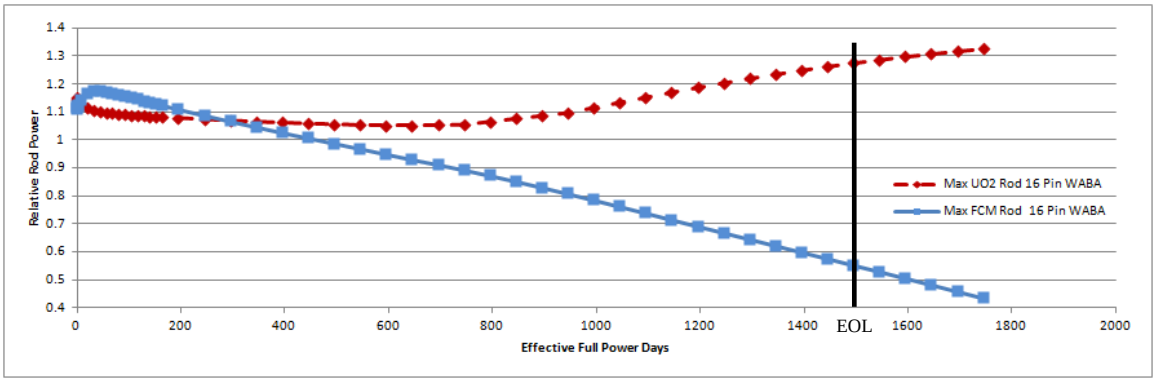

Figure 36 WABA 16 Pin FCM Lattice Max Rod Power

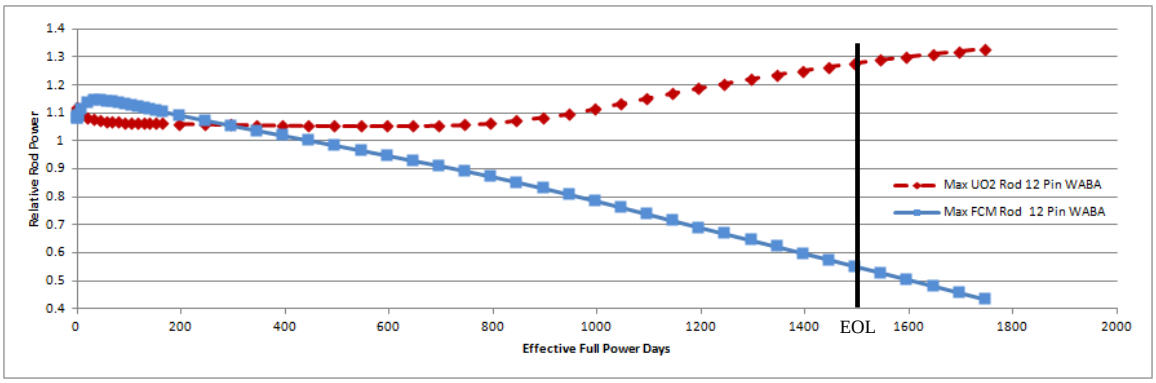

Figure 37 WABA 12 Pin FCM Lattice Max Rod Power

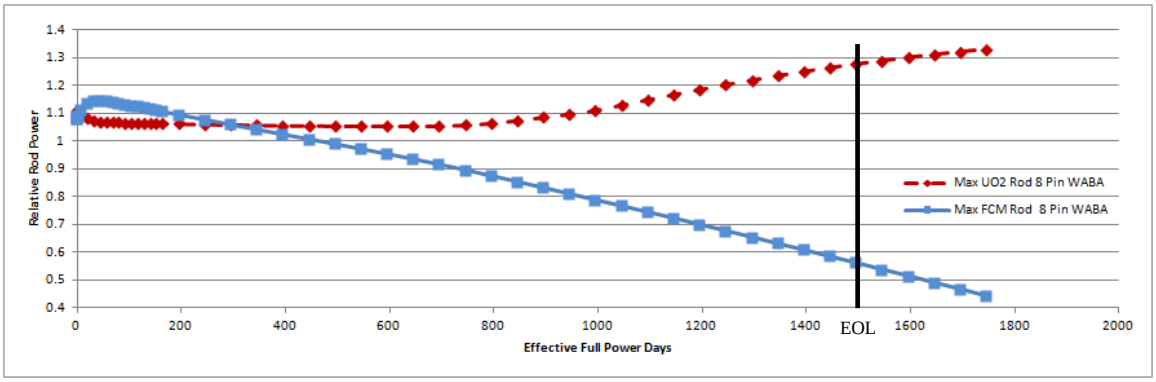

Figure 38 WABA 8 Pin FCM Lattice Max Rod Power

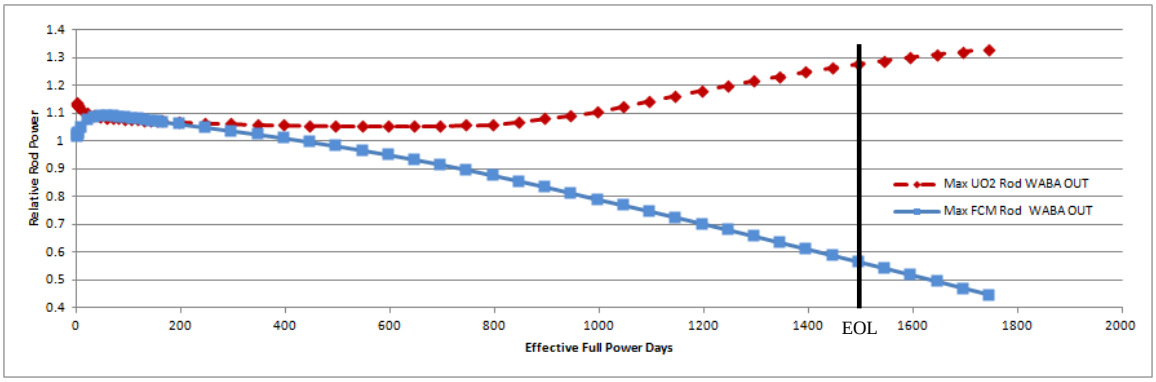

Figure 39 WABA Out FCM Lattice Max Rod Power

Though the early rod peaking for the 24 Pin WABA is high, it is believed that this can be improved by strategically modifying rod enrichments and burnable poison concentrations in the FCM rods, or by using an alternative reactivity hold-down approach (i.e. integral burnable absorbers) without affecting the balance of Pu/Np production to destruction or drastically changing the assembly reactivity profile as a function of burnup.

Based on the relative pin powers and the known time step sizes in the TRITON model, it is possible to calculate the individual rod exposures with respect to average lattice burnup. Figure 40 and Figure 41 indicate that at the anticipated average lattice EOL exposure (i.e. 1500 EFPD or ~70 GWd/MTHM) that the maximum UO_2 rod exposure will be around 60 GWD/MTHM and the maximum FCM rod exposure will be around 670 GWD/MTHM. The maximum UO_2 rod exposure is well within the typical licensed limit of 62 GWd/MTHM for typical UO_2, and the FCM rod exposure is within the expected bunrup tolerance of the FCM fuel of ~750 GWd/MTHM [26,27].

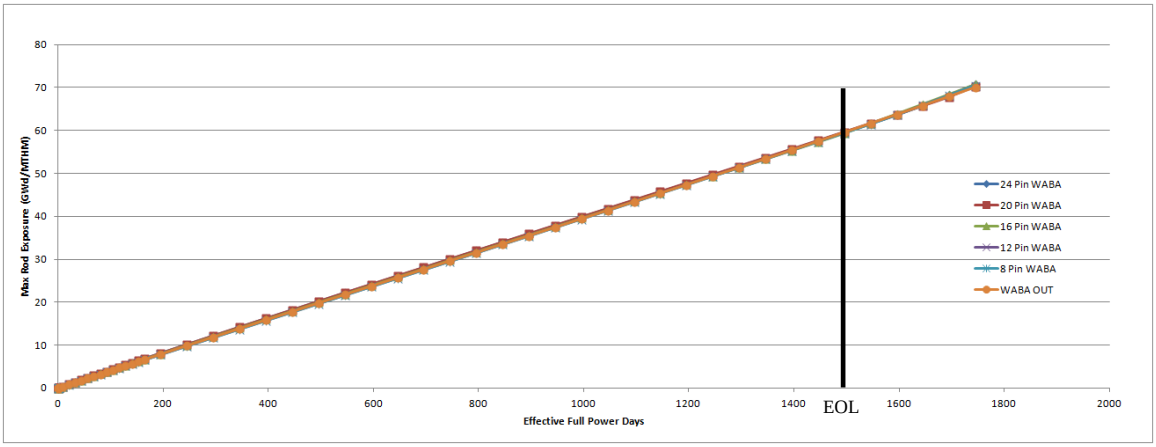

Figure 40 FCM Lattice Maximum UO_2 Rod Burnup

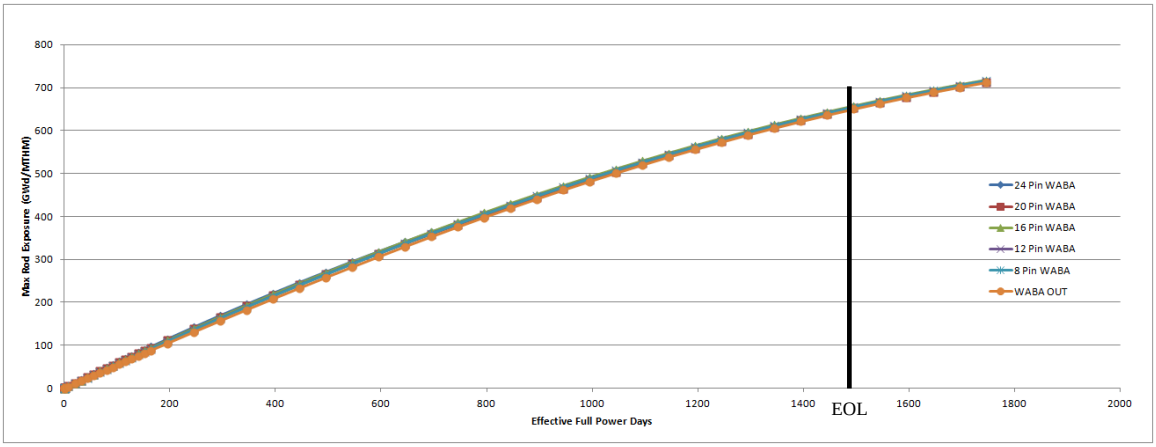

Figure 41 FCM Lattice Maximum FCM Rod Burnup

Table 9 shows that the overall relative percent difference between Pu/Np production and Pu/Np destruction, depending on how long the burnable absorber is left in the assembly, will fall somewhere between -5.5% and -8.2%, which indicates that the assembly very nearly meets the goal of balancing Pu/Np production and destruction (NOTE: a negative value of the net production indicates that more Pu/Np is destroyed than what is created). It should be noted that of the plutonium and neptunium isotopes, only Pu-239 has a net negative value of production. This net destruction of Pu-239 is sufficiently large enough that it over comes the net positive production of the other plutonium and neptunium isotopes.

It should also be noted that the fuel is estimated to have between 6.6% and 7.3% less TRU waste mass than the 4.5% UO_2 lattices when considering the major long lived isotopes shown in Table 9.

Table 9 Total Lattice Mass of Isotopes of Interest at BOL / EOL

		WABA 24 Pin		WABA 20 Pin		WABA 16 Pin		WABA 12 Pin		WABA 8 Pin		WABA OUT	
	nuclide	**BOL**	**EOL**	**BOL**	**EOL**	**BOL**	**EOL**	**BOL**	**EOL**	**BOL**	**EOL**	**BOL**	**EOL**
Mass (g)	**u235**	1.64E+04	2.68E+03	1.64E+04	2.63E+03	1.64E+04	2.59E+03	1.64E+04	2.55E+03	1.64E+04	2.51E+03	1.64E+04	2.42E+03
	u238	3.49E+05	2.68E+03	3.49E+05	2.63E+03	3.49E+05	2.59E+03	3.49E+05	2.55E+03	3.49E+05	2.51E+03	3.49E+05	2.42E+03
	np237	4.00E+02	4.17E+02	4.00E+02	4.17E+02	4.00E+02	4.16E+02	4.00E+02	4.16E+02	4.00E+02	4.15E+02	4.00E+02	4.14E+02
	pu238	2.43E+02	4.21E+02	2.43E+02	4.21E+02	2.43E+02	4.18E+02	2.43E+02	4.16E+02	2.43E+02	4.14E+02	2.43E+02	4.12E+02
	pu239	4.70E+03	2.58E+03	4.70E+03	2.55E+03	4.70E+03	2.52E+03	4.70E+03	2.49E+03	4.70E+03	2.46E+03	4.70E+03	2.41E+03
	pu240	1.78E+03	1.86E+03	1.78E+03	1.86E+03	1.78E+03	1.86E+03	1.78E+03	1.86E+03	1.78E+03	1.86E+03	1.78E+03	1.86E+03
	pu241	4.19E+02	1.17E+03	4.19E+02	1.17E+03	4.19E+02	1.16E+03	4.19E+02	1.15E+03	4.19E+02	1.14E+03	4.19E+02	1.13E+03
	pu242	5.34E+02	1.19E+03	5.34E+02	1.19E+03	5.34E+02	1.19E+03	5.34E+02	1.19E+03	5.34E+02	1.19E+03	5.34E+02	1.20E+03
	cs-137	1.10E-13	9.60E+02	1.10E-13	9.60E+02	1.10E-13	9.61E+02	1.10E-13	9.61E+02	1.10E-13	9.61E+02	1.10E-13	9.61E+02
	ba-137	4.78E-25	4.65E+01	4.65E-25	4.65E+01	4.61E-25	4.65E+01	4.57E-25	4.65E+01	4.55E-25	4.65E+01	4.38E-25	4.66E+01
	sr-90	5.10E-23	3.52E+02	5.11E-23	3.53E+02	5.12E-23	3.54E+02	5.13E-23	3.54E+02	5.15E-23	3.55E+02	5.17E-23	3.56E+02
	y-90	3.72E-24	9.75E-02	3.60E-24	9.77E-02	3.55E-24	9.80E-02	3.49E-24	9.82E-02	3.45E-24	9.84E-02	3.27E-24	9.89E-02
	pr-144	1.04E-26	8.15E-03	1.02E-26	8.15E-03	1.01E-26	8.16E-03	9.99E-27	8.16E-03	9.94E-27	8.16E-03	9.58E-27	8.16E-03
	am-241	1.94E-13	5.19E+01	1.94E-13	5.18E+01	1.94E-13	5.12E+01	1.94E-13	5.07E+01	1.94E-13	5.01E+01	1.94E-13	4.96E+01
	zr-93	7.47E-14	5.03E+02	7.47E-14	5.04E+02	7.47E-14	5.04E+02	7.47E-14	5.05E+02	7.47E-14	5.06E+02	7.47E-14	5.07E+02
	nb-93	7.47E-14	5.84E-05	7.47E-14	5.85E-05	7.47E-14	5.85E-05	7.47E-14	5.85E-05	7.47E-14	5.86E-05	7.47E-14	5.87E-05
	cs-135	1.08E-13	3.68E+02	1.08E-13	3.65E+02	1.08E-13	3.62E+02	1.08E-13	3.59E+02	1.08E-13	3.56E+02	1.08E-13	3.51E+02
	i-129	1.04E-13	1.33E+02	1.04E-13	1.33E+02	1.04E-13	1.33E+02	1.04E-13	1.32E+02	1.04E-13	1.32E+02	1.04E-13	1.32E+02
	tc-99	7.96E-14	5.83E+02	7.96E-14	5.83E+02	7.96E-14	5.84E+02	7.96E-14	5.84E+02	7.96E-14	5.85E+02	7.96E-14	5.85E+02
	np/pu Total	8.08E+03	7.63E+03	8.08E+03	7.60E+03	8.08E+03	7.56E+03	8.08E+03	7.52E+03	8.08E+03	7.48E+03	8.08E+03	7.42E+03
np/pu % Production / Destruction			-5.49%		-5.86%		-6.37%		-6.86%		-7.40%		-8.15%
FCM Waste - UO2 Waste % Diff			-7.26%		-7.14%		-7.04%		-7.00%		-6.87%		-6.60%

3.2. Core Modeling

Core optimization was conducted by means of iteration and reviewing industry designs [26], (NOTE: It was also assumed that no fresh assemblies would be discharged after the first cycle and an additional once burned assembly would be available for placement in the center of the core at the beginning of each cycle). Figure 42 presents a quarter core display of the most optimal equilibrium design and shuffle sequence determined. For the loading plans shown, a 0 indicates a fresh assembly location, a 1 a once-burned assembly, and a 2 a twice-burned assembly. In the WABA pattern, an "N" indicates that no WABA was used in the given assembly, and a number indicates that a WABA with a corresponding number of poison rods was used. Since the reactivity hold-down effects of these absorbers could be duplicated with integral burnable absorbers, the core designs presented did not exclude burnable absorbers from some of the typical control rod locations, though in reality this would not be physically allowable. With regard to the excess reactivity target for these designs, the aim for these designs was to have at least 520 Effective Full Power Days (EFPD) of operation.

WABA Pattern

Row/Column	H	G	F	E	D	C	B	A	
8	N	N	N	N	24	N	16	N	
9	N	24	N	24	N	N	12	N	
10	N	N	24	N	24	N	12	N	
11	N	24	N	N	N	24	12	N	
12	24	N	24	N	N	16	N		
13	N	N	N	24	16	12	N		
14	16	12	12	12	N	N			
15	N	N	N	N					

Control Rod Map

Row/Column	H	G	F	E	D	C	B	A	
8	CD		CA		SD		CC		
9						SB			
10	CA		CC				CB		
11						SC			
12	SD				CD		SA		
13		SB		SC					
14	CC		CB		SA				
15									

Burn Pattern

Row/Column	H	G	F	E	D	C	B	A	
8	1	1	1	1	0	1	0	1	
9	1	0	1	0	1	1	0	2	
10	1	1	0	1	0	1	0	2	
11	1	0	1	1	1	0	0	2	
12	0	1	0	1	1	0	2		
13	1	1	1	0	0	0	2		
14	0	0	0	0	2	2			
15	1	2	2	2					

Shuffle Pattern

Row/Column	H	G	F	E	D	C	B	A	
8	F-10	E-9	G-11	D-8	0	B-8	0	F-10	
9	E-9	0	D-10	0	B-9	B-10	0	C-10	
10	G-11	F-12	0	C-11	0	B-11	0	C-9	
11	H-12	0	E-13	G-9	C-12	0	0	E-10	
12	0	G-14	0	D-13	C-13	0	D-11		
13	H-14	F-14	E-14	0	0	0	D-9		
14	0	0	0	0	E-12	G-12			
15	F-10	F-13	G-13	F-11					

Burn #	Assembly Count
0	76
1	77
2	40

Figure 42 Optimal Equilibrium Fuel Loading and Shuffle Plan (Quarter Core)

Figure 43 provides a plot of the maximum relative peak assembly powers for the equilibrium core design with respect to the number of days of full power operation. This plot shows that assembly relative power peaking is higher than desired (when comparing to typically sought power distributions) , but it is believed from the results that with additional effort and possibly through the implementation of core optimization tools (which were not available for this study), and a more varied selection of assembly types (i.e. greater variety of burnable absorber concentrations) that it is possible to design a core fully loaded with FCM assemblies with a maximum assembly power peaking which is more comparable to what is typically sought in the industry (usually less than or equal to 1.4) [26].

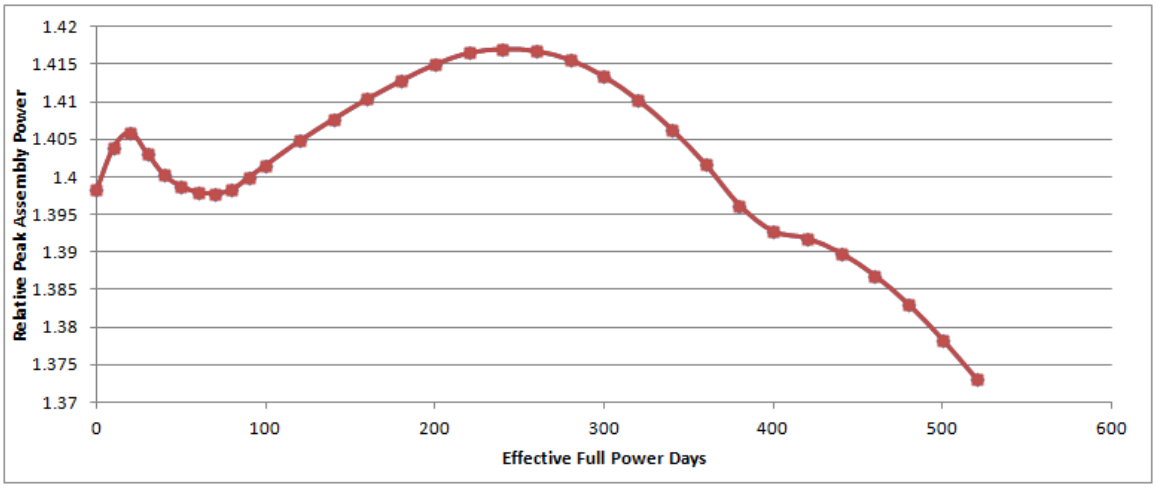

Figure 43 Maximum Relative Assembly Average Power

Figure 44 provides a plot of the calculated All-Rod-Out critical boron concentration (i.e. the boron concentration required to keep the reactor at a critical condition). The point at which the critical boron concentration reaches zero (i.e. the end of possible full power operation and typically considered the end of the operating cycle) corresponds to ~520 days which indicates that the core is capable of operating at full power for the desired cycle length. The peak critical boron concentration is high in comparison to what is normally sought in the industry (approximately 1200 ppm), but it is believed that by using "stronger" poisons (either more concentrated, mixed in with the fuel, or alternative insert design) or by isotopically enriching the core soluble boron that it will be possible to bring this closer to normal levels [26]. An analysis of the Moderator Temperature Coefficient (MTC) feedback at BOC (accomplished by simply increasing and decreasing the inlet coolant temperature by 10°F in the NESTLE model and measuring the associated change in reactivity) shows that the MTC would be approximately -13 pcm/°F. Being that MTC is not expected to become much more

positive than -13 pcm/°F, even with boron concentration increasing to over 1600 ppm, it is reasonable to conclude that the higher than normal boron concentration could be allowable for core operation.

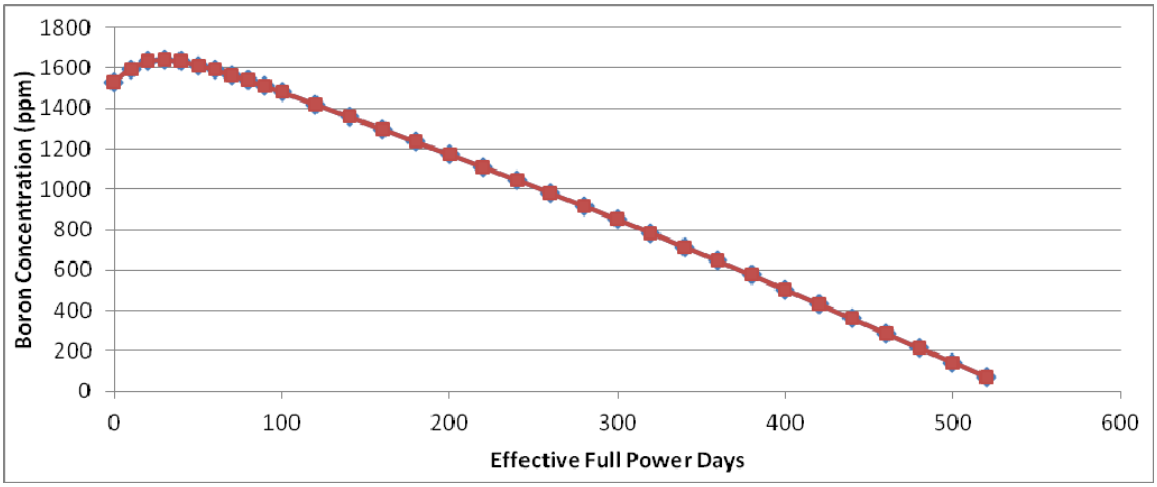

Figure 44 All-Rods-Out Critical Boron Concentration

Figure 45 provides a quarter core display of the Beginning of Cycle (BOC) and End of Cycle (EOC) relative assembly average power distribution and assembly exposures. This shows that the maximum discharge assembly average exposure is 69.32 GWDd/MTHM. Though higher than what is typically seen in the industry, by referring back to the maximum rod burnup plots in Figure 40 and Figure 41 and their associated discussion, it can be seen that the corresponding maximum rod exposure for the UO_2 rods is less than 62 GWd/MTHM limit and the FCM rods is less than 750 GWd/MTHM. As such, the higher assembly average would be acceptable.

BOC Power and Exposures

	H	G	F	E	D	C	B	A
8	1.167	1.161	1.198	1.226	1.398	1.287	1.177	0.485
	33.42	33.83	33.83	34.11	0	30.01	0	33.42
9	1.161	1.287	1.189	1.364	1.318	1.297	1.19	0.36
	33.83	0	34.37	0	30.2	29.49	0	55.32
10	1.198	1.189	1.345	1.256	1.378	1.28	1.095	0.3
	33.83	34.37	0	32.98	0	25.83	0	57.53
11	1.226	1.364	1.256	1.296	1.259	1.154	0.861	0.197
	34.11	0	32.98	31.15	30.19	0	0	60.43
12	1.398	1.318	1.378	1.259	1.261	1.03	0.343	
	0	30.2	0	30.19	23.03	0	58.33	
13	1.287	1.297	1.28	1.154	1.03	0.726	0.184	
	30.01	29.49	25.83	0	0	0	58.82	
14	1.177	1.19	1.095	0.861	0.343	0.184		
	0	0	0	0	58.33	58.82		
15	0.485	0.36	0.3	0.197	Relative Average Assembly Power			
	33.42	55.32	57.53	60.43	Assembly Burnup (GWd/MTHM)			

EOC Power and Exposures

	H	G	F	E	D	C	B	A
8	0.977	0.984	0.993	1.029	1.335	1.057	1.231	0.602
	57.61	58.38	59.09	60.94	34.11	57.76	30.01	46.56
9	0.984	1.291	1.02	1.34	1.077	1.068	1.228	0.472
	58.38	31.15	60.46	33.83	58.82	57.53	30.2	65.38
10	0.993	1.02	1.337	1.045	1.351	1.133	1.224	0.428
	59.09	60.46	33.42	60.43	34.37	55.32	29.49	66.42
11	1.029	1.34	1.045	1.033	1.081	1.373	1.135	0.321
	60.94	33.83	60.43	58.35	58.33	32.98	25.83	66.77
12	1.335	1.077	1.351	1.081	1.157	1.294	0.531	
	34.11	58.82	34.37	58.33	52.62	30.19	69.32	
13	1.057	1.068	1.133	1.373	1.294	1.061	0.33	
	57.76	57.53	55.32	32.98	30.19	23.03	65.14	
14	1.231	1.228	1.224	1.135	0.531	0.33		
	30.01	30.2	29.49	25.83	69.32	65.14		
15	0.602	0.472	0.428	0.321	Relative Average Assembly Power			
	46.56	65.38	66.42	66.77	Assembly Burnup (GWd/MTHM)			

Figure 45 BOC and EOC Relative Assembly Powers and Assembly Exposures

Full core Pu/Np production and destruction was estimated for each assembly by looking up the corresponding SCALE 2D lattice isotopic values associated with each assembly's BOC and EOC exposures. Using this approach, the percent difference in Pu/Np production minus destruction at end of cycle was estimated to be nearly -1.85%, implying a reasonable balance between production and destruction of the Pu/Np inventory at EOC.

4. Conclusions

The presented fuel assembly design demonstrated, by means of SCALE simulation, a similar reactivity behavior as a typical UO_2 design, a peak relative rod power higher than the desired maximum of 1.2 but not so high as to necessarily be prohibitive, and a near balance of Pu/Np production and destruction. The presented core design, by means of NESTLE, was shown to meet a 520 day cycle length, have a peak relative assembly power comparable to the industry typical maximum values of 1.4, have a peak critical boron concentration higher than what is typically seen in the industry but not unacceptably so, and have maximum rod burnups less than the legal UO_2 limit and anticipated FCM limit. It is believed from these results that FCM fuels can play a role in the recycling of Pu/Np material in LWRs. They demonstrate the possibility of designing fuel and core designs that neutronically operate in a manner very similar to how typical fuel and core designs behave whilst recycling a substantial amount of Plutonium and Neptunium waste material (especially Pu-239).

Though these results indicate similar behavior and the potential for further optimization of the fuel and core designs, certain code/method improvements will be necessary should one wish to realistically design fuel and cores for use in the commercial industry. The error associated with using the RPT method and the lack of NESTLE accounting for history effects, though small enough for scoping studies such as what is presented in this document, would be unacceptable in terms of industry expectations of modeling accuracy [28]. Furthermore, the prohibitively slow execution times associated with a true DH calculation in TRITON are not conducive towards the fuel optimization

process, which is often times a practice of trial and error. In the case of TRITON, the BRANCH function support would need to be added for DH geometry modeling so that lattice cross-section data could be generated without employing the RPT method. Also, the ASSIGN function support would need to be added to drastically reduce the run time of these models so as to make TRITON more favorable to the optimization process. For NESTLE, some improvements to the code will be required to account for history effects, but this should be relatively easy upgrade to implement. Also, the addition of a cross-section library enrichment/reactivity interpolation/extrapolation feature would provide a user the ability to experiment with different assembly enrichments/reactivities in the core design process without requiring full 2-D lattice model calculations should the desired assembly enrichment/reactivity to be tried fall somewhere between or beyond the already available cross-libraries. This addition would greatly help reduce the amount of time spent performing core optimizations as well as reduce the amount of 2-D lattice model calculations required as part of the trial and error process.

Concerning further core and fuel optimization, it is expected that by employing a diversity of different fuel and core design technique (i.e. strategic rod by rod enrichment loading, use of fuel integral poison as opposed to WABAs, and assembly batching) that much improved fuel and core designs can be achieved. Also, using a combination of computer automated intelligent optimizers, which are commonly employed in the industry, along with the previously stated code runtime improvements one would expect to quickly converge on improved designs that should perform at least as well as current operating fuel and core designs.

Other studies and future work that should be pursued beyond this report are the designing of assemblies and cores in which greater than balanced Pu/Np destruction is achieved, as well as the investigation of other safety and performance values of interest (ex: temperature coefficients, shutdown margin, reactivity excursions and accident analysis). Additionally, research will be required in regards to Pu/Np FCM fuel fabrication and irradiation behavior. For eventual use in commercial reactors, design licensing and lead test rods / assemblies will also be required.

References

1. M. Visosky, Y. Shatilla, P. Hejzlar, M. S. Kazimi, "Actinide Transmutation in PWRs Using CONFU Assemblies", *Nuclear Science and Engineering,* **Vol. 163**, pp.215-242 (2009)

2. Gilles Youinou and Alfredo Vasile, "Plutonium Multirecycling in Standard PWRs Loaded with Evolutionary Fuels", *Nuclear Science and Engineering,* **Vol. 151**, pp.25-45 (2005)

3. "Physics of Plutonium Recycling: Volume VI Multiple Plutonium Recycling in Advanced PWRs", OECD/NEA, 2002.

4. Denise Grubert, "Nuclear Reprocessing in the US: A Levelized Cost Analysis" Masters Project, Duke University, August 2009

5. "Spent Fuel Reprocessing Options", IAEA, Vienna, Austria, August 2008, IAEA-TECDOC-1587

6. C. Rodriguez, A. Baxter, D. McEachern, M. Fikani, and F. Venneri, "Deep-Burn: Making Nuclear Waste Transmutation Practical," *Nuclear Engineering and Design,* **222**, 299 (2003)

7. "Deep-Burn Modular Helium Reactor Fuel Development Plan", General Atomics and Oak Ridge National Laboratory, September 2002, GA-244-0-TRT-000167, ORNL/TM-2002/135

8. Rodney D. Hunt and Jack L. Collins, "Uranium kernel formation via internal gelation", Radiochimica Acta, **92** (2004) pg 909

9. "S. Bresnick, "MHTGR Fuel Process and Quality Control Description," DOE-HTGR-90257, Rev. 0, General Atomics, September 1991

10. K.A. Terrani, J.O. Kiggans, Y. Katoh, K. Shimoda, F.C. Montgomery, B.L. Armstrong, C.M. Parish, T. Hinoki, J.D. Hunn, L.L. Snead, "Fabrication and Characterization of Fully Ceramic Microencapsulated Fuels", *J. Nucl. Mater.*, http://dx.doi.org/10.1016/j.jnucmat.2012.03.049, (2012)

11. F. Venneri, Y. Kim, L.L. Snead, K.A. Terrani, A. Ougouag, J.E. Tulenko, C.W. Forsberg, P.F. Peterson, E.J. Lahoda, "Fully Ceramic Microencapsulated Fuels: A Transformational Technology for Present and Next Generation Reactors -a Preliminary Analysis of FCM Fuel Reactor Operation," *Transactions of the American Nuclear Society*, Hollywood, Florida, **104**, (2011) pg 671

12. S.G. Hong, F. Venneri, K.H. Lee, J.Y. Cho, S.Y. Park, C.K. Jo, "Physics Characteristics Evaluation of Fuel Assemblies using FCM (Fully Ceramic Micro-encapsulated) Fuel for the Deep Burn Management of Transuranics in LWRs," *Transactions of the American Nuclear Society*, Washington, D.C., **105**, pg 777, Oct. 30 - Nov. 3, 2011

13. "Pressurized Water Reactor (PWR) Systems", Reactor Concepts Manual, USNRC Technical Training Center, 0603. http://www.nrc.gov/reading-rm/basic-ref/teachers/04.pdf

14. "Watts Bar Unit 2 Final Safety Analysis Report (FSAR)", Amendment 93, Section 4, ML091400651, April 30, 2009. http://adamswebsearch2.nrc.gov/idmws/ViewDocByAccession.asp?AccessionNumber=ML091400651

15. R.J. Ellis, "System Definition Document: Reactor Data Necessary for Modeling Plutonium Disposition in Catawba Nuclear Station", Computational Physics and Engineering Division at Oak Ridge National Laboratory, ORNL/TM-1999/255, September 2000

16. "Scale: A Comprehensive Modeling and Simulation Suite for Nuclear Safety Analysis and Design", ORNL/TM-2005/39, Version 6.1, June 2011. Available from Radiation Safety Information Computational Center at Oak Ridge National Laboratory as CCC-785

17. M.A. Jessee, M.D. DeHart, "TRITON: A Multipurpose Transport, Depletion, and Sensitivity and Uncertainty Analysis Module", ORNL/TM-2005/39, Version 6.1, Oak Ridge National Laboratory, June 2011

18. S. Goluoglu, D.F. HollenBach, L.M. Petrie, "CSAS6: Control Module for Enhanced Criticality Safety Analysis with KENO-VI", ORNL/TM-2005/39, Version 6.1, Oak Ridge National Laboratory, June 2011

19. "NESTLE: Code System to Solve the Few Group Neutron Diffusion Equation Utilizing the Nodal Expansion Method (NEM) for Eigenvalue, Adjoint, and Fixed-Source Steady-State and Transient Problems," Version 5.2.1, June 2003. Available from Radiation Safety Information Computational Center at Oak Ridge National Laboratory as CCC-641

20. J.J Duderstadt, L.J. Hamilton, "Nuclear Reactor Analysis", John Wiley & Sons, Inc., United States, 1976. ISBN 0-471-22363-8

21. Hermilo Hernandez Noyola, "Pin-Wise Loading Optimization and Lattice-to-Core Coupling for Isotopic Management in Light Water Reactors", PhD Dissertation, University of Tennessee, 2010

22. Yonghee Kim and Min Baek, "Elimination of Double Heterogeneity through a Reactivity-Equivalent Physical Transformation", *Proceeding of GLOBAL 2005*, Tsukuba, Japan, Oct 9-13, 2005, Paper No. 548

23. T. Kozlowski, T. Downar, "PWR MOX/UO_2 Core Transient Benchmark" OECD/NEA, NEA No. 6048, January 2007

24. T. M. Besmann, "Thermochemical assessment of oxygen gettering by SiC or ZrC in PuO_{2-x} TRISO fuel", *Journal of Nuclear Materials*, **397**, pg 69-73, 2010

25. F. Ganda, E. Greenspan, "Plutonium recycling in hydride fueled PWR cores", *Nuclear Engineering and Design*, **239**, pg 1489 - 1504, 2009

26. "Sequoyah HTP Fuel Transition (NP)", AREVA NP Inc., ANP-2986(NP), Rev. 002, June 2011

27. Yonghee Kim, Francesco Venneri, "Optimization of One-Pass Transuranic Deep Burn in a Modular Helium Reactor", *Nuclear Science and Engineering*, **160**, pg 59 - 74, 2008

28. "Technical Specifications Sequoyah Nuclear Plant Unit No. 01", U.S. Nuclear Regulatory Commission, Docket No. 50-327, NUREG-0658, Rev.1, Fall 1980

29. "Destruction rate analysis of transuranic targets in sodium-cooled fast reactors (SFR) assemblies using MCNPX and SCALE 6.0", *Progress in Nuclear Engineering*, **52**, pg 387-394, 2010

Vita

Cole Gentry was born April 30, 1985 in Chattanooga, Tennessee. Cole attended the Notre Dame High School in Chattanooga and graduate in May of 2003. Cole then attended the University of Tennessee in Knoxville where he studied Nuclear Engineering. During his undergraduate career, Cole worked several semester as an intern with the Tennessee Valley Authority (TVA) in the Nuclear Fuels Design group at the Chattanooga corporate offices, as well as the Balance of Plant and Reactor Engineering groups at the Sequoyah Nuclear Facility. Cole graduated May 2008 Summa Cum Laude and was one of four top undergraduates in the College of Engineering.

After graduating, Cole went to work as a Reactor Engineer at the TVA Sequoyah Nuclear Facility for two years before deciding to return to academia to pursue an advanced degree. Cole currently attends the University of Tennessee and works as a research assistant on collaborative projects between the Oak Ridge National Laboratory and the University of Tennessee. He will obtain his Masters Degree the spring of 2012 and will continue onward towards his Ph.D. Eventually, Cole wishes continue into a career of both research and teaching as a professor.